Investigation on the Differences in the Mechanical Properties of Fresh, Frozen, and Vitrified Porcine Menisci

by

Junran Sun

A thesis submitted in partial fulfillment of the requirements for the degree of

Master of Science

in

Structural Engineering

Department of Civil and Environmental Engineering
University of Alberta

ABSTRACT

The medial and lateral menisci are two semilunar-shaped fibrocartilaginous tissues in the knee that serve multiple important biomechnical functions. While removal of the menisci leads to progressive degenerative changes in the knee, meniscal transplantation is explored to restore normal knee biomechanics. Preservation and long-term storage of meniscal allografts would improve the availability of the tissue for transplantation. One of the most common meniscal preservation approaches in clinical practice is freezing, but it has the limitation of destroying viable cells and causing tissue deformation due to the formation of ice crystals. On the other hand, vitrification, the transformation of an aqueous solution into a non-crystalline amorphous solid without nucleating ice during the cooling and warming process, is being explored. Numerous studies in the literature have quantified the mechanical properties of the meniscal tissue under tension and compression. Nevertheless, the majority of the studies have concentrated on the comparison of the tensile mechanical properties along the longitudinal and radial orientations, and there have been no published studies exploring the effect of vitrification on either the tensile or compressive mechanical properties of the meniscal tissue to date. Therefore, the primary objective of this research is to investigate the differences in the tensile mechanical properties along the circumferential-peripheral, circumferential-central, longitudinal, and radial orientations and the compressive mechanical properties in the axial direction of fresh, frozen, and vitrified porcine lateral menisci. The secondary objective of this research is to investigate the variations in the tensile mechanical properties of the meniscus along the four different orientations (i.e. circumferential-peripheral, circumferential-central, longitudinal, and radial). Quasi-static tensile testing and unconfined compressive stress-relaxation testing were conducted to quantify the

mechanical properties of fresh, frozen, and vitrified porcine lateral menisci. One-way analysis of variance (ANOVA) with linear contrasts was performed for the evaluation of statistical significance and a p-value < 0.05 was accepted as significant. Experimental results indicated that fresh and vitrified menisci exhibit comparable mechanical properties, whereas frozen menisci exhibit inferior mechanical properties in comparison with fresh and vitrified menisci. Furthermore, superior ultimate tensile stress and failure strain were found along the circumferential-peripheral orientation, while inferior ultimate tensile stress and tensile modulus were found along the radial orientation. Besides, the mean tensile modulus along the circumferential (central and peripheral) and longitudinal orientations are approximately twofold to fourfold higher than that along the radial orientation. The findings of this research revealed that vitrification is superior to freezing in preserving mechanical properties of the meniscal tissue, vitrification is hence likely to be a competitive alternative to freezing for meniscal transplantation in the future.

PREFACE

This thesis is an original work by Junran Sun. The research project, of which this thesis is a part, received research ethics approval from the University of Alberta Research Ethics Office under the Exceptions to the Requirement for ACUC Review.

ACKNOWLEDGMENTS

I would like to express my deepest gratitude to my supervisors, Dr. Samer Adeeb, Dr. Gail Thornton, and Dr. Lindsey Westover, who guided and encouraged me through each stage of the research. This research could not have been accomplished without their continuous support, infinite patience, enthusiastic participation, and invaluable input.

I would like to show my sincere appreciation to Dr. Nadr Jomha for his persistent support, immense knowledge, and insightful comments throughout this research.

I would like to acknowledge Leila Laouar and Kezhou Wu for their generous assistance in the lab and constructive recommendations for this research.

Last but not the least I wish to thank my family, especially Chenxi, for providing me with great love and unfailing spiritually support throughout these years.

Funding for this research project is provided by the Edmonton Orthopaedic Research Committee (EORC) and the Natural Science and Engineering Research Council of Canada (NSERC).

TABLE OF CONTENTS

LIST OF TABLES

LIST OF FIGURES

Chapter 1: Introduction

1.1 Background

The menisci are two crescent-shaped fibrocartilaginous structures interposed between the femoral condyles and the tibial plateau of each knee joint. Mechanically, the meniscus can be considered as a biphasic medium composed of a solid phase and a fluid phase (Kelly et al., 1990). Histologically, the meniscus is a complex fibrocartilaginous tissue composed primarily of an interlacing network of collagen fibers (Kelly et al., 1990) that are predominantly oriented circumferentially. Both the medial and lateral menisci are integral consituents of a normally functioning knee that perform several crucial biomechnical functions including load transmission, shock absorption, joint stability, and joint lubrication and nutrition. Meniscal tears are one of the most frequent injuries to the knee. Different treatment options for meniscal tears include nonoperative management, surgical repair, meniscectomy, and meniscal transplantation. Meniscal tears within the peripheral vascularized zone can be treated with nonoperative treatment or surgical repair (Miller III & Azar, 2007). For instances in which tears are incapable of healing and total meniscectomy is necessary, meniscal replacement via allograft transplantation is undergoing extensive research in an effort to restore normal knee biomechanical functions and prevent progressive joint degeneration. Fresh allografts provide undamaged viable cells and may be the ideal type of transplant. However, the availability of a fresh allograft is limited by the high risk of infectious disease transmission and the short time-frame (up to 7 days) required between the donor death and implantation (Fabbriciani et al., 1997; Junkin et al., 2009). The availability of the meniscal allografts is increased with the technique of freezing; however, the cell viability cannot

be retained and the collagen architecture is altered severely (Gelber et al., 2008). In comparison with freezing, cryopreservation has the ability to preserve partial cell viability against the formation of ice crystals. Recent studies by Gelber et al. (2009) and Jacquet et al. (2018) demostrated that cryopreservation is superior to freezing in keeping meniscal collagen network intact and preserving meniscus histologic ultrastructure.

Conventional cryopreservation, accomplished with the use of a slow freezing rate and cryoprotective agents, involves the formation of ice crystals during the freezing process but restricts the ice to the less damaging extracellular space of the tissue (Finger & Bischof, 2018). Nevertheless, ice formation is lethal to cells (Mcgann & Farrant, 1976; Jomha et al., 2012; Fahy & Wowk, 2015) and causes severe alteration in the structural architecture of the matrix (Jomha et al., 2004; Gelber et al., 2008). In an attempt to overcome these issues and successfully cryopreserve architecturally complex tissues, vitrification, an alternative approach to conventional cryopreservation, is being explored. Vitrification refers to the transformation of an aqueous solution into a non-crystalline amorphous solid or glass without nucleating ice during the cooling and warming process (Jomha et al., 2012). Vitrification is typically achieved by cooling the substance below the glass transition temperature with the presence of a rapid cooling rate and high concentrations of cryoprotective agents (Fahy et al., 1984). Specifically, tissues are often plunged in liquid nitrogen (-196 ℃) to reach a rapid cooling rate of approximately 200 ℃$/min$ (Sakai & Engelmann, 2007). As the viscosity of the solution reaches a sufficiently high value during the cooling process, crystallization of ice is inhibited (Pegg & Diaper, 1990) by the formation of an amorphous solid. For transplantation purposes, preservation of biological substances at cryogenic

temperatures via vitrification is theoretically indefinite since translational molecular motions are remarkably arrested (Fahy et al., 1984), making all biological and chemical activities effectively ceased (Jomha et al., 2012). Vitrification thus becomes a promising meniscal preservation method.

Many studies have characterized the tensile and compressive mechanical properties of the meniscal tissue. While frozen porcine menisci are commonly used in quantifying mechanical properties of the menisci (Sweigart et al., 2004; Gabrion et al., 2005; Stapleton et al., 2007; Abdelgaied et al., 2015; Lakes et al., 2016), there has been limited emphasis on fresh porcine menisci. The tensile mechanical properties of the meniscal tissue vary with respect to the orientation. The majority of the studies investigating the orientational variations in the tensile mechanical properties of the meniscal tissue have focused on the comparison between the longitudinal and radial directions (Proctor et al., 1989; Tissakht & Ahmed, 1995; Lakes et al., 2016; Peloquin et al., 2016) and demonstrated that the tensile modulus of the tissue in the longitudinal direction can be sixfold to tenfold higher than that in the radial direction. Since the collagen fibers within the meniscal tissue are predominantly oriented circumferentially, the tensile mechanical properties of specimens along the circumferential orientation with maximized circumferential collagen fibers are worth exploring. Furthermore, only a small portion of the studies have investigated the effect of preservation techniques on the tensile mechanical properties of the meniscal tissue. Arnoczky et al. (1988) evaluated the effect of cryopreservation on the tensile mechanical properties of canine menisci and indicated no statistically significant differences on the tensile mechanical properties between fresh and short-term cryopreserved (1 week) menisci. A more recent study by Ahmad et al. (2017) investigated the differences in the tensile mechanical

properties between frozen and cryopreserved human menisci and reported a significantly higher ultimate tensile stress of cryopreserved menisci. Therefore, the researchers concluded that cryopreservation is a better preservation technique in comparison with freezing.

1.2 Objectives

The primary objective of this research is to investigate the differences in the tensile and compressive mechanical properties of fresh, frozen, and vitrified porcine lateral menisci. Specifically, the tensile mechanical properties are quantified along four different orientations including circumferential-peripheral, circumferential-central, longitudinal, and radial orientations (Figure 1-1). Moreover, the compressive mechanical properties are quantified in the axial direction (Figure 1-2). The primary hypothesis is that fresh and vitrified porcine menisci would exhibit comparable mechanical properties, whereas frozen menisci would exhibit inferior mechanical properties in comparison with fresh and vitrified menisci.

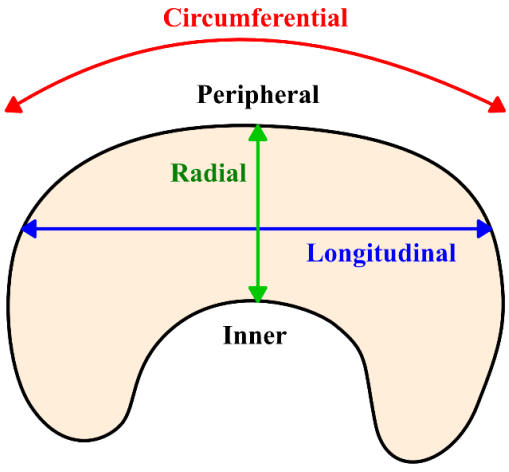

Figure 1-1: A Schematic Illustrating the Circumferential, Longitudinal, and Radial Orientations

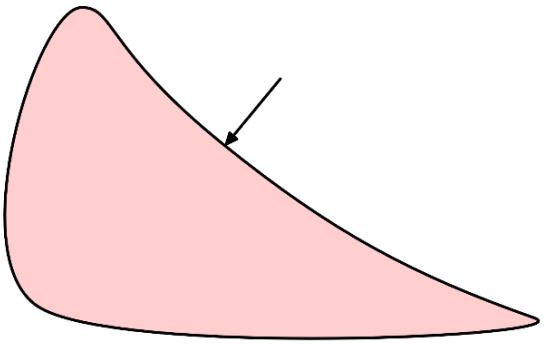

Figure 1-2: A Schematic Illustrating the Axial Direction

The secondary objective of this research is to investigate the variations in the tensile mechanical properties of the meniscus along four different orientations (i.e. circumferential-peripheral, circumferential-central, longitudinal, and radial). The secondary hypothesis is that specimens along the circumferential-peripheral orientation would exhibit superior tensile mechanical properties in comparison with specimens along the three other different orientations (i.e. circumferential-central, longitudinal, and radial), whereas specimens along the radial orientation would exhibit inferior tensile mechanical properties in comparison with specimens along the three other orientations (i.e. circumferential-peripheral, circumferential-central, and longitudinal).

1.3 Research Contribution

There have been numerous attempts in the literature to quantify the mechanical properties of the meniscal tissue under tension and compression. Nevertheless, there has been limited attention on the mechanical properties of fresh porcine menisci and the majority of studies have concentrated on the comparison of tensile mechanical properties along the longitudinal and radial orientations.

Moreover, while only a small portion of the studies have investigated the effect of freezing and conventional cryopreservation approaches on the tensile mechanical properties of the meniscal tissue, there have been no published studies demonstrating the effect of vitrification on either the tensile or compressive mechanical properties of the meniscal tissue to date. Therefore, this research involves the investigation on the differences in the tensile mechanical properties along four different orientations (i.e. circumferential-peripheral, circumferential-central, longitudinal, and radial) and the differences in the compressive mechanical properties in the axial direction of fresh, frozen, and vitrified porcine lateral menisci.

The findings of this research demonstrate a great potential for vitrification to become an alternative approach in cryopreserving the meniscal tissue for transplantation purposes. If vitrification is superior in preserving mechanical properties of the tissue, retaining structural architecture of the matrix, and lowering the risk of tearing in comparison with freezing in future research, then vitrification could emerge as a superior approach in preserving the meniscal tissue and patients undergoing total meniscectomy would be presented with an attractive alternative for meniscal transplantation.

1.4 Outline of Thesis

This thesis consists of 6 chapters.

Chapter 1 provides the background and objectives of the research topic and original contributions to knowledge in the field of research.

Chapter 2 provides a review of the literature in the field comprising anatomy and ultrastructure of the meniscus, biomechanical functions of the meniscus, meniscal tear and repair, meniscal preservation techniques, and behaviour of the meniscus under tension and compression.

Chapter 3 presents the testing method for conducting the experiments, which encompasses the preparation procedure of testing specimens, the testing protocols for unconfined compressive stress-relaxation testing and quasi-static tensile testing, the determination of compressive and tensile mechanical properties, and the evaluation of statistical significance.

Chapter 4 presents the experimental results including the compressive mechanical properties in the axial direction, the tensile mechanical properties along the circumferential-peripheral, circumferential-central, longitudinal, and radial orientations, and the orientational variations in the tensile mechanical properties.

Chapter 5 provides a detailed discussion of the major findings.

Chapter 6 provides the conclusion with respect to the objectives, limitations of this research, and considerations for future research.

Chapter 2: Literature Review

2.1 The Meniscus

2.1.1 Anatomy

The concave proximal surfaces of the menisci enable effective articulation with the corresponding convex femoral condyles, while the flat distal surfaces accommodate to the tibial plateau (Allen et al., 1995; Brindle et al., 2001). The thick and convex peripheral edge of each meniscus is attached to the inside capsule of the joint, whereas the inner edge tapers to a thin free edge (Arnoczky, 1990).

The medial and lateral menisci are wedge-shaped in cross-section and are crucial to the long-term health of the knee. The medial and lateral menisci are histologically similar but structurally unique with different shapes, sizes, and attachments (Allen et al., 1995). The medial meniscus is crescentic in shape and is significantly broader posteriorly and progressively becomes narrower approaching to the anterior horn (Allen et al., 1995). The lateral meniscus is more circular in shape and has a more uniform width in comparison with the medial meniscus, with the anterior and posterior horns in relatively close proximity (Allen et al., 1995). Moreover, the lateral meniscus covers a larger portion of the tibial plateau than the medial meniscus (Arnoczky, 1990). In addition, the peripheral edge of the medial meniscus is firmly attached to the joint capsule and less mobile compared with the lateral meniscus (Kawamura et al., 2003).

2.1.1.1 Porcine Menisci

The porcine meniscus is a practical and economically feasible model commonly used in investigating meniscal ultrastructure, biomechanics, material properties, preservation techniques, and treatment options for evaluation and development of human meniscal repairing (Takroni et al., 2016). A recent study by Takroni et al. (2016) compared the weight, volume, and dimensions of human menisci with porcine menisci. In summary, Takroni and coworkers found that the average weight and volume of porcine menisci are significantly larger than human menisci, and the lateral meniscus has greater weight and volume in comparison with the medial meniscus from the same species. The dimensions of the porcine meniscus are significantly greater than the human meniscus, with the exception of the circumference. Specifically, the average measurement ratio of the porcine lateral meniscus to the human lateral meniscus is 1.4: 1. Moreover, the average measurement ratio of the porcine medial meniscus to the human medial meniscus is 1.3: 1 and the horizontal width of the porcine medial meniscus is significantly greater than the human medial meniscus in the anterior and middle regions. Furthermore, no statistically significant differences were identified on the dimensions between the human medial and lateral menisci. By contrast, the porcine lateral meniscus exhibits significantly greater dimensions in comparison with the medial meniscus except for the circumference.

2.1.2 Ultrastructure

Histologically, the meniscus is a complex fibrocartilaginous tissue composed primarily of an interlacing network of collagen fibers interposed with cells that are responsible for synthesizing and maintaining the extracellular matrix comprising proteoglycan molecules and glycoproteins

(Kelly et al., 1990). The meniscus can be considered as a biphasic medium composed of a solid phase (collagen, proteoglycans, and other non-collagenous proteins) and a fluid phase (water and interstitial electrolytes) (Kelly et al., 1990). The collagen fibers within the meniscal tissue are specifically arranged to convert axial compression forces into circumferential or "hoop" stresses (Brindle et al., 2001). The alignment of the collagen fibers varies with respect to the depth in the tissue, comprising of three layers (superficial, lamellar, and deep) that describe the tissue from surface to core (Sanchez-Adams & Guilak, 2013). In the superior superficial layer, the collagen fibers are amorphous and oriented randomly, whereas in the inferior superficial layer, the collagen fibers are more arranged in a radial patten (Sanchez-Adams & Guilak, 2013). Amorphous collagen organization persists through the lamellar layer and random fiber orientation dominates the layer with radially oriented short fibers existing only on the periphery and at the horns of the meniscus (Sanchez-Adams & Guilak, 2013). In the deep layer, the collagen fibers are predominantly arranged circumferentially with a few radially orientated fibers interwoven between the circumferential fibers (Fithian et al., 1990). The orientation of the collagen fibers appears to be directly related to the function of the meniscus (McDermott et al., 2010). The circumferential fibers allow the meniscus to function as a load transmitter and withstand the tension (Arnoczky, 1990). The radial fibers interwoven between the circumferential fibers may act as tie fibers to provide structural integrity and resist longitudinal splitting of the meniscus (Bullough et al., 1970).

2.1.3 Biomechanical Functions

The biomechanical functions of the meniscus reflect its anatomy, ultrastructure, and relationship to the surrounding intra-articular and extra-articular structures (Allen et al., 1995). The

biomechanical functions performed by the menisci include load transmission, shock absorption, joint stability, and joint lubrication and nutrition.

2.1.3.1 Load Transmission

The meniscus is compressed and tends to be extruded peripherally as axial loads are generated across the knee during weight bearing. The firm attachments to the tibia through the anterior and posterior insertional ligaments prevent the excessive peripheral extrusion of the meniscus during weight bearing (McDermott et al., 2008). The axial compression forces are transmitted from the femur via the menisci to the tibia and converted into "hoop" (circumferential) stresses, causing tension along the circumferential collagen fibers within the meniscal tissue (McDermott et al., 2008). The lateral meniscus carries 70% of the joint load in the lateral compartment while the medial meniscus carries 50% of the joint load in the medial compartment (Seedhom et al., 1974). After total meniscectomy, the tibia-femoral contact area is decreased by approximately 75% and the peak contact stress is increased by approximately 235% (Baratz et al., 1986). Such significant increase in the stress leads to accelerated articular cartilage damage and early degenerative changes (Mccarty et al., 2002; Kawamura et al., 2003). Thus, the menisci function as a load transmitter, protecting the articular cartilage from excessive stresses and preventing early degeneration in the knee (Allen et al., 1995).

2.1.3.2 Shock Absorption

The viscoelastic behaviour of the menisci may serve to attenuate the shock waves produced by impulse loading of the knee (Voloshin & Wosk, 1983; Boyd & Myers, 2003). The axially directed energy is absorbed by the collagen fibers (solid phase) and is further absorbed by the expulsion of the interstitial fluid (fluid phase) out of the tissue as the tissue being compressed (McDermott et al., 2008). After meniscectomy, the shock-absorbing capacity of the knee is reduced by approximately 20%, which may eventually lead to the development of degenerative osteoarthritis (Voloshin & Wosk, 1983). Contrarily, Andrews and coworkers (2011) proposed that the hypothesis of the menisci acting as a shock absorber in the knee is inconclusvie and unsupported by the literature.

2.1.3.3 Joint Stability

The concave proximal surface and flat distal surface of the meniscus conform respectively to the femoral condyles and the tibial plateau, and the wedged-shape structure of the meniscus contributes to its function in joint stability (Kawamura et al., 2003). Axial loading of the knee with intact menisci has a multidirectional stabilizing function, which limits excess motion in all directions (Arnoczky, 1992, as cited in Fox et al., 2011). The medial meniscus serves as a secondary stabilizer of particular importance in an anterior cruciate ligament (ACL) deficient knee, restricting the anterior tibial displacement (Levy et al., 1982). Medial meniscectomy in the ACL intact knee has a minor effect on the anterior-posterior displacement of the tibia on the femur (Levy et al., 1982). Nevertheless, the medial meniscus is prone to injury in the ACL deficient knee and

medial meniscectomy in the ACL deficient knee leads to a significant increase in the anterior tibial displacement (Levy et al., 1982).

2.1.3.4 Joint Lubrication and Nutrition

The menisci contribute significantly to joint conformity which promotes the viscous hydrodynamic action required for fluid-film lubrication, assisting in the overall lubrication of the articular cartilage surfaces of the knee (Arnoczky & McDevitt, 2000, as cited in Kawamura et al., 2003). During weight bearing, the synovial fluid may be extruded into the articular cartilage, reducing frictional forces and thus aiding in joint lubrication (Arnoczky et al., 1988, as cited in Fox et al., 2011). Furthermore, it has been suggested that total meniscectomy may lead to an approximately 20% increase in friction (MacConaill, 1932).

The menisci also aid in the nutrition of the knee. A system of canals adjacent to the blood vessels within the substance of the meniscus communicates with the synovial cavity and may provide an additional means of transporting synovial fluid through the meniscus for nutritional purposes (Bird & Sweet, 1987). The peripheral portion of the meniscus is likely to receive nutrition from the vasculature at the periphery of the meniscus (Allen et al., 1995), whereas the inner portion of the meniscus is likely to receive nutrition from synovial fluid diffusion, the synovial cavity, or mechanical pumping secondary to joint motion (Arnoczky et al., 1987, as cited in Allen et al., 1995).

2.2 Meniscal Tear and Repair

2.2.1 Meniscal Tear

The medial meniscus is less mobile and more susceptible to injuries in comparison with the lateral meniscus (Majewski et al., 2006). Meniscal tears may be classified on the basis of the tear pattern seen at arthroscopy or on the etiology of the meniscal injury (Greis et al., 2002). Common meniscal tear patterns involve vertical longitudinal (including bucket-handle), horizontal, radial, complex, and degenerative tears. The most common meniscal tears are degenerative or complex tears in older patients and traumatic vertical longitudinal tears in the young patients (Lopez-Vidriero & Johnson, 2012). Another means of classifying meniscal tears is based on the anatomical location of a tear relative to the blood supply of the meniscus (Lopez-Vidriero & Johnson, 2012), which determines the potential for healing after meniscal repair. Meniscal tears in the peripheral vascularized zone (red-red tears) has the best healing prognosis (Rath, 2000); tears at the border of the vascularized zone (red-white tears) have sufficient vascularity to theoretically heal by fibrovascular proliferation; tears in the inner avascular zone (white-white tears) are incapable of healing and meniscectomy can be considered as a rational treatment (Lopez-Vidriero & Johnson, 2012).

2.2.2 Meniscal Repair

The key factors in determining the treatment to meniscal injuries are accessibility of cells and inflammatory mediators to the location of the tear (Rath, 2000). Different treatment options for meniscal tears include nonoperative management, surgical repair, meniscectomy, and meniscal

transplantation. Meniscal tears occur in the peripheral vascularized zone with infrequent and minimal symptoms can be treated with nonoperative treatment such as rehabilitation and restricted activity (Miller III & Azar, 2007). Nevertheless, chronic tears superimposed with an acute meniscal injury may require surgical repair (Miller III & Azar, 2007). Surgical repair is suitable for tears within the peripheral one-fourth to one-third of the meniscus since here the vascularized zone is capable of providing the sutured tear with vascular granulation tissue that results in healing of the tear (Miller III & Azar, 2007). Total meniscectomy can lead to development of degenerative changes in the knee (Fairbank, 1948; Cox et al., 1975). Techniques of partial meniscectomy and surgical repair have limited the cases of total meniscectomy. However, there are instances in which total meniscectomy of the meniscus is the only option, and thus meniscal transplantation or tissue-engineered meniscus is being explored (Kawamura et al., 2003).

2.3 Meniscal Preservation Techniques

The effects of meniscal preservation techniques and storage time on the biological and biochemical integrity of the tissue may affect the success of a meniscal transplant in clinical practice (Fabbriciani et al., 1997). Aside from using fresh allografts, the available meniscal preservation techniques include freezing and cryopreservation.

2.3.1 Fresh

Fresh allografts may be the ideal type of transplant since fresh tissue provides undamaged viable cells and a viable chondrocyte population may contribute in maintaining the extracellular matrix

as well as the mechanical integrity of the allograft after transplantation (Arnoczky & Milachowski, 1990; Siegel & Roberts, 1993, as cited in Rijk, 2004). However, the availability of a fresh allograft is limited in clinical practice. To maintain the cell viability, the application of fresh transplantation requires a short time-frame (up to 7 days) between donor death and implantation (Fabbriciani et al., 1997; Junkin et al., 2009). Furthermore, the clinical applicability of fresh allografts may be limited by the high risk of infectious disease transmission as applying secondary sterilization techniques will destroy any viable cells (Junkin et al., 2009). Besides, thorough serologic evaluation of the allograft and matching the meniscal size of donor to receiver commonly require more than 7 days, after which the viability of meniscal fibrochondrocyte cannot be retained (Junkin et al., 2009).

2.3.2 Freezing

Freezing of the meniscal allograft to −80°C destroys viable cells of connective tissue completely and denatures histocompatibility antigens, minimizing the likelihood of provoking an immune response when being transplanted (Brown & Cruess, 1982, as cited in Rijk, 2004). Furthermore, the risk of infectious disease transmission is low with the possibility of applying secondary sterilization techniques (Arnoczky, 1992, as cited in Mickiewicz et al., 2014). Salai et al. (1996) demonstrated that the freezing process causes severe cellular damage while properties of the collagen network are retained. Conversely, a more recent study reported that the freezing process alters the collagen network of the meniscus (Gelber et al., 2008), and this severe alteration in the collagen architecture may cause the meniscus to be more susceptible to injury (Arnoczky et al., 1992).

2.3.3 Cryopreservation

Cryopreservation is accomplished with the use of a slow freezing rate and cryoprotective agents (such as dimethyl sulfoxide and glycerol) in an attempt to partially preserve cell viability by maintaining cell membrane integrity (Mazur, 1970) against the formation of ice crystals. The percentage of viable cells after cryopreservation ranges from 10% to 30% (Arnoczky et al., 1988; Verdonk & Kohn, 1999). According to a more recent study, an even wider range of cell survival after cryopreservation has been observed from 4% to 54% (Gelber et al., 2009). Nevertheless, the percentage of cell survival declines with storage time (Arnoczky et al., 1988). Additionally, the risk of infectious disease transmission may increase since secondary sterilization techniques that affect cell viability are not applicable (Rijk, 2004). Furthermore, cryopreservation does not alter the meniscal ultrastructure and biomechanical properties although the cellular viability is unpredictable (Gelber et al., 2009).

In comparison with freezing, cryopreservation is able to keep partial cell viability due to the use of cryoprotectant agents. An experimental study in goats suggested that no significant differences in morphological and biochemical characteristics could be found between cryopreservation and freezing, and these characteristics of meniscal allografts may not be improved by the presence of residual viable cells (Fabbriciani et al., 1997). Conversely, recent studies demonstrated that cryopreservation is superior to freezing in keeping meniscal collagen network intact and preserving meniscus histologic ultrastructure (Gelber et al., 2009; Jacquet et al., 2018).

2.4 Material Properties of Meniscal Tissue

Biomechanically, the meniscal tissue exhibits complex material properties which are inhomogeneous (location dependent), anisotropic (direction dependent), viscoelastic (rate or time dependent), and nonlinear (Sanchez-Adams & Guilak, 2013). The meniscus can be considered as a biphasic medium composed of a solid phase (collagen, proteoglycans, and other non-collagenous proteins) and a fluid phase (water and interstitial electrolytes) (Kelly et al., 1990). The viscoelastic behaviour of the meniscus can be described by the biphasic theory (Sanchez-Adams & Guilak, 2013). The biphasic theory states that the intrinsic properties of the collagen-proteoglycan solid matrix in conjunction with interstitial fluid flow govern the deformability of the hydrated soft tissue (Kelly et al., 1990). The deformation of the solid matrix leads to the elastic response, whereas the transient fluid flowing through the porous-permeable solid matrix results in the viscous response (Kelly et al., 1990). Therefore, the viscoelastic behaviour of the meniscus is primarily attributed to the interaction between the solid phase and fluid phase.

The mechanical properties of the meniscus can be characterized by tensile and compressive testing. Owing to the variation in the collagen alignment and the asymmetrical shape of the meniscus, characterization of the mechanical properties of the meniscal tissue involves spatially variated specimens, orientating along and perpendicular to the direction of collagen alignment (Sanchez-Adams & Guilak, 2013).

2.4.1 Behaviour in Tension

The tensile properties of the meniscal tissue vary with respect to the orientation (circumferential and radial), the region (anterior, central, posterior), and the layer (superficial, middle, and deep). Twelve studies in the literature have been reviewed and are summarized in Table 2-1, including the specimen species, specimen variation, specimen preparation, and loading protocol. The specimen dimensions and loading protocol used in this research are designed on the basis of previous studies (Anderson et al., 1993; Goertzen et al., 1997; Abdelgaied et al., 2015; Lechner et al., 2000; Lakes et al., 2016) and sufficient pilot experiments. The tensile mechanical testing is further explained in Chapter 3 Methods.

Table 2-1: Twelve Studies – Tensile Testing Review

Study	Species	Variation	Specimen Preparation			Loading Protocol	
Arnoczky et al. (1988)	Canine	Circumferential	Storage:	Cryopreserved		Preload:	1 g
			Slicing:	Microtome			
			Dimension:	Width:	~1 mm	Precondition:	5 g
				Thickness:	400 μm		10 $cycles$
				Length:	1.5 – 2 mm	Loading Rate:	
			Die Cutter:	A razor blade die			
Proctor et al. (1989)	Bovine	Circumferential Radial	Storage:	Frozen		Preload:	1 gf
	Medial		Slicing:	Microtome			
		Anterior Posterior	Dimension:	Width:		Precondition:	5 gf
				Thickness:	400 μm		10 $cycles$
		Surface Middle Deep		Length:	5 mm	Loading Rate:	0.05 cm/min (0.00167 $/s$)
			Die Cutter:	Specially designed razor blade die			
Anderson et al. (1993)	Ovine	Circumferential	Storage:	Frozen		Preload:	2 g
	Medial		Slicing:	Microtome			
			Dimension:	Width:	3 mm	Precondition:	3% $strain$
				Thickness:	350 μm		10 $cycles$
				Length:	8 mm	Loading Rate:	0.5 mm/min (0.002 $/s$)
			Die Cutter:	Cutting jig			

Study	Species	Variation	Specimen Preparation			Loading Protocol	
Skaggs et al. (1994)	Bovine	Radial	Storage:	Frozen		Preload:	0.01 N
	Medial	Anterior Central Posterior	Slicing:	Microtome			
			Dimension:	Width:	1 mm	Precondition:	0.05 N
				Thickness:	400 μm		10 $cycles$
				Length:	1 – 5 mm	Loading Rate:	0.005 $/s$
			Die Cutter:	Specially designed razor blade die			
Tissakht & Ahmed (1995)	Human	Circumferential Radial	Storage:	Frozen		Preload:	
	Medial Lateral		Slicing:	Scalpel			
		Anterior Central Posterior	Dimension:	Width:	1.75 – 3 mm	Precondition:	
				Thickness:	0.8 – 2 mm		
				Length:	5.5 – 8 mm	Loading Rate:	$5 \pm 1\%/min$
		Surface Middle Deep	Die Cutter:				
Goertzen et al. (1997)	Bovine	Longitudinal Isotropic Transverse Oblique	Storage:	Fresh		Preload:	0.05 N
	Medial		Slicing:	Microtome			
			Dimension:	Width:	2.6 mm	Precondition:	
				Thickness:	0.75 mm		
				Length:	8 mm	Loading Rate:	0.01 mm/s (0.002 $/s$)
			Die Cutter:	Specially constructed cutting die			
Lechner et al. (2000)	Human	Circumferential	Storage:	Fresh		Preload:	0.05 N
	Medial	Anterior Central Posterior	Slicing:	Microtome			
			Dimension:	Width:	1.0 mm	Precondition:	0.01 mm/s to 3% $strain$
				Thickness:	0.5, 1.5, 3.0 mm		10 $cycles$
				Length:	10 mm	Loading Rate:	0.006 mm/s
			Die Cutter:	Specially designed razor blade die			
Stapleton et al. (2007)	Porcine	Circumferential	Storage:	Frozen		Preload:	0.02 N
	Medial		Slicing:				
			Dimension:	Width:	1.5 mm	Precondition:	
				Thickness:	6 μm		
				Length:	3 mm	Loading Rate:	3 mm/min
			Die Cutter:				
Abdelgaied et al. (2015)	Porcine	Circumferential	Storage:	Frozen		Preload:	0.5 N
	Medial		Slicing:	A custom tissue cutter			
			Dimension:	Width:	1.5, 2.0, 3.0 mm	Precondition:	
				Thickness:	1.5, 2.0, 3.0 mm		
				Length:	10 mm	Loading Rate:	1 mm/min (0.00167 $/s$)
			Die Cutter:				

Study	Species	Variation	Specimen Preparation			Loading Protocol	
Peloquin et al. (2016)	Bovine	Circumferential Radial	Storage:	Frozen		Preload:	20 kPa
	Medial Lateral		Slicing:	Microtome			
			Dimension:	Width:	3 – 5 mm	Precondition:	4% $strain$
				Thickness:	1 – 2 mm		10 $cycles$
				Length:	8 – 15 mm	Loading Rate:	0.5 mm/s
			Die Cutter:	Biopsy punch			
Lakes et al. (2016)	Porcine	Circumferential Radial	Storage:	Frozen		Preload:	0.05 N
	Medial		Slicing:	Parallel blades			
			Dimension:	Width:	2 mm	Precondition:	Cir: 10 $cycles$ of 0.65% $strain$
				Thickness:	450 μm		Rad: 10 $cycles$ of 2.5% $strain$
				Length:	3.7 mm	Loading Rate:	Cir: 10 $cycles$ of 1.3% $strain$ at 0.26 $\%/s$
			Die Cutter:	Custom dumbbell shaped punch			Rad: 10 $cycles$ of 5% $stain$ at 1 $\%/s$
Ahmad et al. (2017)	Human	Circumferential	Storage:	Frozen	Cryopreserved	Preload:	Not specified
	Medial Lateral		Slicing:	Blade		Precondition:	
			Dimension:	Not specified		Loading Rate:	
			Die Cutter:				

2.4.1.1 Anatomical and Orientational Differences

The human lateral meniscus exhibits a higher tensile modulus (ranging from 159 MPa to 294 MPa) in comparison with the medial meniscus (ranging from 93 MPa to 159 MPa) (Fithian et al., 1990). Tissakht and Ahmed (1995) also studied human menisci and reported that the average tensile modulus of the lateral meniscus (11.64 MPa) in the radial direction is higher than that of the medial meniscus (9.94 MPa). Likewise, the average tensile modulus of the lateral meniscus (111.66 MPa) in the circumferential direction is higher than that of the medial meniscus (82.98 MPa).

Several studies demonstrated that the tensile modulus of the tissue in the circumferential direction can be sixfold to tenfold higher than that in the radial direction (Proctor et al., 1989; Tissakht & Ahmed, 1995; Lakes et al., 2016; Peloquin et al., 2016).

2.4.1.2 Regional Variations

A trend is observed toward increasing tensile stiffness of human menisci in the circumferential direction from anterior to posterior (Fithian et al., 1990). Proctor et al. (1989) found that circumferential posterior specimens from the interior zone of the bovine meniscus are significantly stiffer than similar anterior specimens. Skaggs et al. (1994) observed that specimens comprised of full radial tie fibers are stiffest and proposed that the abundance of radial tie fibers in the posterior region of the bovine meniscus may contribute to the increased stiffness of this region. On the other hand, Tissakht and Ahmed (1995) indicated that regional variation has a significant effect only on the maximum stress for human radial specimens, whereas no significant effect of regional variation is found for circumferential specimens. Moreover, a study of human medial meniscus by Lechner et al. (2000) indicated no significant effect of either the circumferential or radial location of the specimens on the tensile modulus, while a superior mean tensile modulus for the anterior region was reported compared with that for the central or posterior region of the meniscus. Furthermore, Fithian et al. (1990) demonstrated that specimens from the peripheral two-thirds of the bovine medial meniscus are significantly stiffer than specimens from the inner one-third of the meniscus.

2.4.1.3 Layer Inhomogeneities

Layer inhomogeneities are present in the tensile material properties with respect to the distance from the femoral surface (Proctor et al., 1989). Proctor et al. (1989) demonstrated that the femoral surface of the canine meniscus is isotropic in tension, whereas the interior of the meniscus is anisotropic where the circumferential specimens are much stiffer than the radial specimens. For radially oriented specimens, the tensile modulus was found to decrease significantly from approximately $71.4\ MPa$ in the superficial layer to $2.8\ MPa$ in the middle layer, and increase slightly to $4.6\ MPa$ in the deep layer (Proctor et al., 1989). Moreover, an investigation by Tissakht and Ahmed (1995) confirmed that the average tensile modulus of radially oriented specimens from the middle layer is significantly less stiff than that of specimens from the superficial and deep layers. For circumferential orientated specimens, the tensile modulus was found to increase significantly from approximately $48.3\ MPa$ in the superficial layer to $198.4\ MPa$ in the middle layer, and decrease significantly to $139.0\ MPa$ in the deep layer (Proctor et al., 1989). Conversely, Tissakht and Ahmed (1995) indicated that the average tensile modulus of circumferentially oriented specimens from the middle layer is less stiff compared with that of specimens from the superficial and deep layers.

Additionally, a study of human medial meniscus by Lechner et al. (2000) indicated that the circumferential tensile modulus of the meniscus is inversely dependent on the specimen thickness and proposed that testing a specimen with small cross-sectional area may overestimate the effective modulus of the meniscus on the whole.

2.4.2 Behaviour in Compression

The compressive properties of the meniscal tissue vary with respect to the orientation (circumferential and radial) and the region (anterior, central, posterior). Nine studies in the literature have been reviewed and are summarized in Table 2-2, including the specimen species, testing method, specimen variation, and specimen preparation. The compressive testing protocol used in this research is designed on the basis of preliminary experiments and is further explained in Chapter 3 Methods.

Table 2-2: Nine Studies - Compression Testing Review

Study	**Species**	**Testing**	**Variation**		**Specimen Preparation**		
Proctor et al. (1989)	Bovine	Confined	4 Regions	Anterior	Storage:	Frozen	
	Medial			Central-Anterior	Die Cutter:	A sharply tapered hollow drill bit	
				Central-Posterior			
				Posterior	Slicing:	Microtome	
			2 Depths	Superficial, Deep	Dimension: (Disc)	Diameter:	6.35 mm
			1 Orientation	Axial		Thickness:	1 mm
Leslie et al. (2000)	Human	Unconfined	2 Regions	Central-Anterior	Storage:	Fresh	
	Medial Lateral			Central-Posterior	Die Cutter:		
			3 Orientations	Circumferential	Slicing:	Two parallel microtome blades	
				Radial	Dimension: (Rectangular)	Area:	20.68 – 84.48 $mm2$
				Axial		Thickness:	0.89 – 2.69 mm
Sweigart et al. (2004)	6 Animals	Indentation	3 Regions	Anterior	Storage:	Frozen	
	Medial			Central	Die Cutter:	Each Region	
				Posterior	Slicing:		
			2 Depths	Femoral	Dimension:		
				Tibial			
			1 Orientation	Axial			

Study	Species	Testing	Variation		Specimen Preparation		
Gabrion et al. (2005)	Porcine	Unconfined	3 Orientations	Circumferential	Storage:	Frozen	
	Medial Lateral			Radial	Die Cutter:		
				Axial	Slicing:		
					Dimension: (Cubic)	Area:	33.15 mm^2
Sweigart & Athanasiou (2006)	Rabbit	Indentation	3 Regions	Anterior	Storage:	Frozen	
	Medial			Central	Die Cutter:	Each Region	
				Posterior	Slicing:		
			2 Depths	Femoral	Dimension:		
				Tibial			
			1 Orientation	Axial			
Chia & Hull (2008)	Human	Unconfined	3 Regions	Anterior	Storage:	Frozen	
	Medial			Central	Die Cutter:	A custom cutting device	
				Posterior			
			2 Orientations	Axial	Dimension: (Cubic)	Edge length:	2 mm
				Radial			
Bursac et al. (2009)	Human	Unconfined	3 Regions	Anterior	Storage:	Frozen	
	Medial Lateral			Central	Die Cutter:	A biopsy punch	
				Posterior	Slicing:	Custom-made parallel blades	
			1 Orientation	Axial	Dimension: (Disc)	Diameter:	3.9 mm
						Thickness:	1.8 mm
Abdelgaied et al. (2015)	Porcine	Unconfined	3 Regions	Anterior	Storage:	Frozen	
	Medial			Central	Die Cutter:		
				Posterior	Slicing:		
			1 Orientation	Axial	Dimension: (Disc)	Diameter:	8 mm
						Thickness:	3 mm
Lakes et al. (2016)	Porcine	Unconfined	1 Region	Central	Storage:	Frozen	
	Medial		1 Orientation	Axial	Die Cutter:	A biopsy punch	
					Slicing:	Parallel blades	
					Dimension: (Disc)	Diameter:	5 mm
						Thickness:	3.5 mm

2.4.2.1 Anatomical and Orientational Differences

In several studies of human and porcine menisci, no significant differences in Young's modulus between lateral and medial menisci were reported (Leslie et al., 2000; Gabrion et al., 2005). By contrast, Bursac et al. (2009) found that the anterior region of the medial meniscus is significantly stiffer than that of the lateral meniscus, whereas the posterior region of the medial meniscus is significantly less stiff than that of the lateral meniscus.

The response of the meniscal tissue to unconfined compression is anisotropic (Leslie et al., 2000; Gabrion et al., 2005). Leslie et al. (2000) indicated that the meniscal tissue is significantly stiffer in response to axial compressive forces than to radial or circumferential forces. Moreover, Gabrion et al. (2005) reported that the meniscal tissue is twice as stiff in the axial direction than in the radial or circumferential directions.

2.4.2.2 Regional Variations

A study of bovine medial meniscus by Proctor et al. (1989) demonstrated that the deep layer of the meniscus exhibits a highly significant regional variation, in which deep posterior specimens are significantly stiffer than deep anterior and central-anterior specimens. Conversely, Sweigart et al. (2004) noted significant intraspecies and interspecies variations in the creep indentation compressive properties among the six topographical locations, with the highest compressive modulus occurred in the anterior region of the meniscus. In particular, specimens from the femoral-anterior region of the porcine meniscus are stiffest while specimens from the tibial-anterior region

is statistically stiffer than specimens from the tibial-posterior region (Sweigart et al., 2004). Moreover, specimens from the anterior region of the human meniscus including both the femoral and tibial sides are significantly stiffer than specimens from the central or posterior regions (Sweigart et al., 2004). A study of human medial menisci by Chia and Hull (2008) confirmed that the modulus in the anterior region is significantly greater than that in the posterior region. Furthermore, Bursac et al. (2009) demonstrated that the anterior region of the medial meniscus is significantly stiffer than the central and posterior regions, whereas no significant effect of regional variation is found on the stiffness of the lateral meniscus although an upward trend is observed from the anterior to posterior regions.

2.5 Summary

The review of the literature encompasses anatomy and ultrastructure of the meniscus, biomechanical functions of the meniscus, meniscal tear and repair, meniscal preservation methods, and behaviour of the meniscus under tension and compression. The understanding of the meniscal ultrastructure helps to establish the hypothesis regarding the orientational variations in the tensile mechanical properties. The background knowledge of various preservation methods has motivated and informed the research on investigating the differences in the mechanical properties between the fresh menisci and menisci preserved by freezing and vitrification, providing a strong support for establishing the primary hypothesis. Furthermore, the review of the literature on the behaviour of the meniscus under tension and compression builds the basis for designing the testing protocols used in this research and creates a baseline for comparisons between the experimental results from

this research and findings in the literature. In addition, the summary of the existing studies on the mechanical properties of the meniscus reveals the limitations in the field of research.

Chapter 3: Methods

3.1 Specimen Preparation

In this research, porcine knee joints were purchased at a local grocery store and were stored at 4 ℃ prior to use. Porcine knee joints were disarticulated in the laboratory (Figure 3-1). Only lateral menisci were used for testing with the intention of limiting the manipulated variable only to the choice of meniscal preservation techniques. Lateral menisci were separated from surrounding ligamentous structures and bony attachments (Doral et al., 2018) using a surgical blade and were immersed in 1X phosphate-buffered saline (PBS) to remove excess blood. Lateral menisci exhibiting visual evidence of injury or degeneration were discarded. After dissection, lateral menisci were incubated in PBS + antibiotics (100 $units/ml$ penicillin, 100 $\mu g/ml$ streptomycin, and 0.25 $\mu g/ml$ amphotericin B) solution at room temperature for 20 minutes. Tensile testing groups for each orientation (i.e. circumferential-peripheral, circumferential-central, longitudinal, radial) consisted of 18 porcine lateral meniscal samples that were separated equally into three groups ($n = 6$ per group), namely, fresh, frozen, and vitrified. Likewise, compression testing groups consisted of 36 porcine lateral meniscal samples that were separated equally into three groups ($n = 12$ per group). Subsequently, each sample in the fresh group was assigned an identification number randomly and was stored in Dulbecco's modified eagle medium (DMEM) supplemented with 20% fetal calf serum (FCS) at 4 ℃ until the day of mechanical testing (Verdonk et al., 2005; Verdonk et al., 2006). The frozen group and the vitrified group were placed in DMEM at 4 ℃ while waiting for treatments.

Figure 3-1: Medial (Left) and Lateral (Right) Menisci in a Porcine Knee Joint

3.1.1 Treatment Protocol

The samples waiting for treatments in each group were whole lateral menisci. The treatment protocol of the frozen group was designed on the basis of the patent by Brockbank (1992). The treatment protocol of the vitrified group was designed on the basis of studies by Takroni et al. (2017) and Wu et al. (2018).

3.1.1.1 Frozen Group

Each sample in the frozen group was transferred to a $50\,mL$ tube with $40\,mL$ DMEM supplemented with 10% FCS, $1M$ dimethyl sulfoxide (DMSO), and 2.5% chondroitin sulfate. After being assigned an identification number randomly, each sample was placed in a basket filled with ice. The basket was then placed on an orbital shaker at a speed of $180\,rpm$ for 30-minute shaking at 4 ℃. Afterwards, each sample was moved to the freezer and was frozen to -80 ℃ at a cooling rate of approximately 0.5 ℃$/min$. Once the temperature inside the tube reached -80 ℃, each sample was moved to liquid nitrogen (-196 ℃) for storage prior to mechanical testing.

3.1.1.2 Vitrified Group

Each sample in the vitrified group was transferred to a $50\,mL$ tube with $40\,mL$ DMEM supplemented with $3M$ ethylene glycol (EG) and was placed on an orbital shaker at a speed of $180\,rpm$ for 180-minute shaking at room temperature. After being assigned an identification number randomly, each sample was transferred to a $50\,mL$ tube with $40\,mL$ DMEM supplemented with $4M$ DMSO and $4M$ EG, and was placed in -5 ℃ alcohol bath for 15-minute

stirring. Subsequently, each sample was moved to liquid nitrogen (-196 ℃) for storage prior to mechanical testing.

3.1.1.3 Sample Warming

On the day of testing, frozen and vitrified samples were taken out of the liquid nitrogen and were thawed in a warming bath at 37 ℃ until all cryoprotectant agents (CPAs) (i.e. DMSO for the frozen group; DMSO and EG for the vitrified group) exhibited visual evidence of melting.

3.1.1.4 Sample Washing

After all CPAs had melted, each frozen or vitrified sample was transferred to a 150 mL beaker with 25 mL DMEM (4 ℃) and was washed using an orbital shaker at a speed of 180 rpm for 30-minute shaking at 4 ℃. In this manner, two more washes were repeated to remove all CPAs from each sample.

3.1.2 Compression Specimens

Specimens for compression testing were harvested from the central-posterior region of each lateral meniscus (Figure 3-2). A 6 mm diameter biopsy punch was oriented perpendicular to the femoral surface to punch out a cylindrical core. The oblique tibial surface was trimmed to be parallel to the femoral surface with a surgical blade. After trimming, two parallel cuts separated 2 mm apart were made at the mid-depth of the cylindrical core to create a 2 mm thick cylindrical specimen (Figure 3-3). The diameter and thickness of each compression specimen were designed based on the

preliminary experiments. In this manner, a total of 36 cylindrical specimens were harvested from 36 porcine lateral menisci ($n = 12$ per group). Each of these specimens was stored in a $50\ mL$ tube with DMEM at 4 ℃ prior to compression testing.

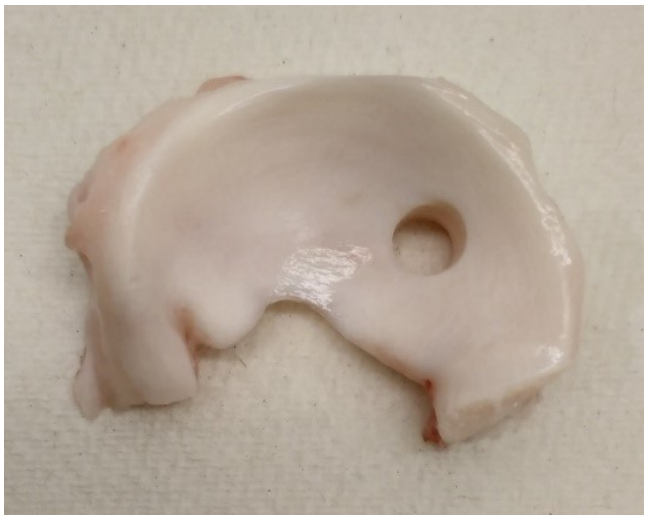

Figure 3-2: A Compressive Specimen Harvested from Central-Posterior Region of Each Lateral Meniscus

Figure 3-3: A Cylindrical Compressive Specimen

3.1.3 Tensile Specimens

Specimens for tensile testing were harvested from the central region of each lateral meniscus along four different orientations (Figure 3-4): circumferential-peripheral, circumferential-central, longitudinal, and radial orientations.

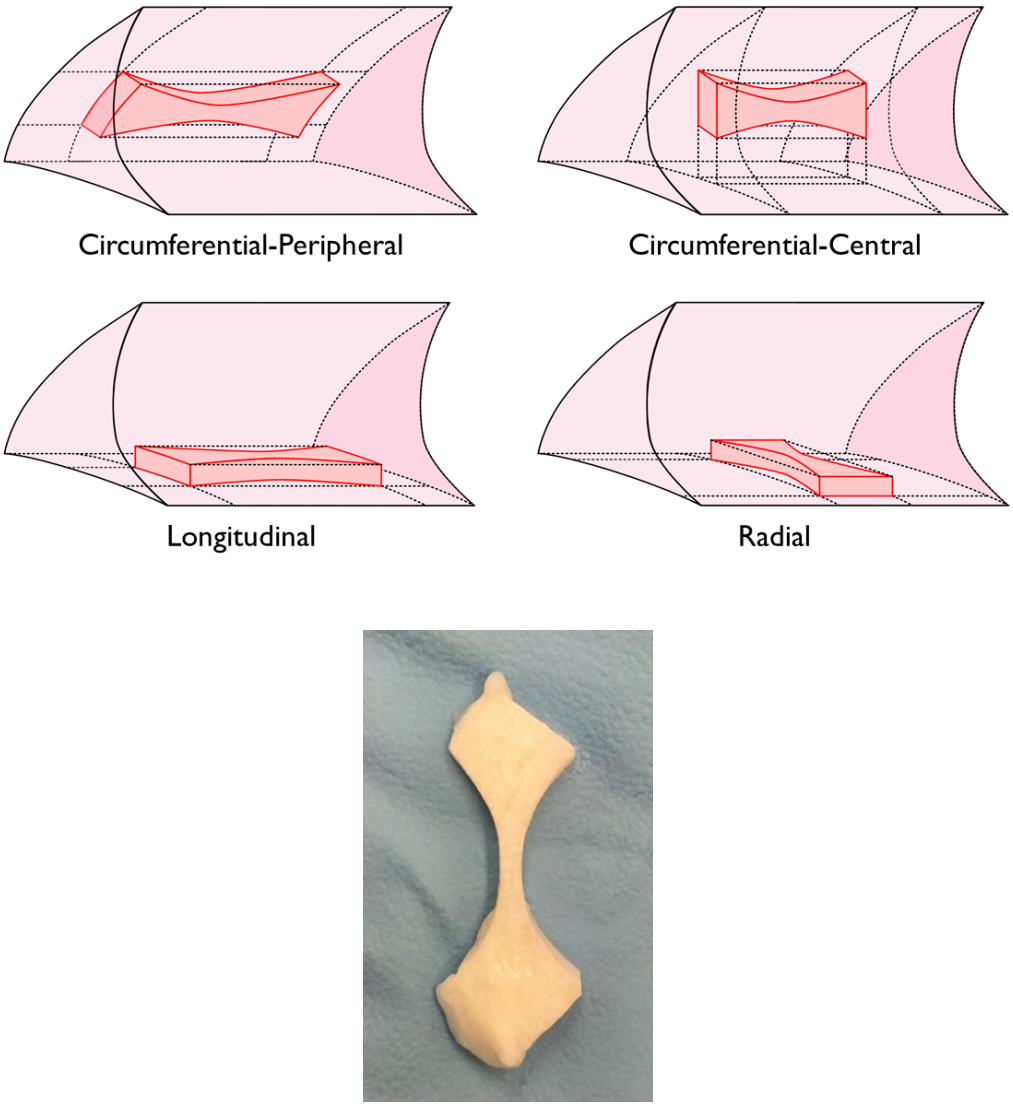

Figure 3-4: A Dumbbell-Shaped Tensile Specimen Harvested from Central Region of Each Lateral Meniscus along 4 Different Orientations

3.1.3.1 Circumferential-Peripheral Orientation

Circumferential-peripheral specimens were harvested parallel to the circumferential collagen fibres at the peripheral edge from the central region of each lateral meniscus (Figure 3-5). Initially, a thin slice was removed at the peripheral edge with a surgical blade orientated perpendicular to the tibial surface to create a flat incision. Subsequently, a single $2\ mm$ thick slice of tissue was cut parallel to the peripheral incision and was placed, on the sectioned side, on a specially constructed cutting die (Goertzen, 1992) (Figure 3-6) to stamp out a dumbbell-shaped testing specimen with a $2\ mm$ gauge width. The thickness and width of each tensile specimen were designed based on the preliminary experiments and literature review (Table 2-1). In this manner, the circumferential collagen fibres in each circumferential-peripheral specimen were maximized. A total of 18 dumbbell-shaped circumferential-peripheral specimens were harvested from 18 porcine lateral menisci ($n = 6$ per group). Each of these specimens was stored in a $50\ mL$ tube with DMEM at 4 ℃ prior to tensile testing.

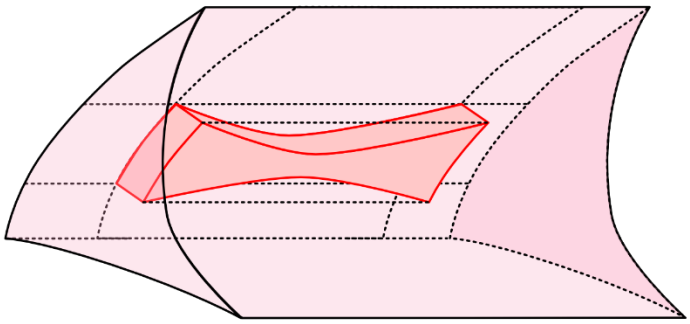

Figure 3-5: A Schematic Illustrating the Circumferential-Peripheral Specimen

Figure 3-6: A Specimen Placed on a Specially Constructed Cutting Die

3.1.3.2 Circumferential-Central Orientation

Circumferential-central specimens were harvested along the circumferential orientation from the central region of each lateral meniscus (Figure 3-7). Initially, serial slices were made starting at the inner rim with a surgical blade oriented perpendicular to the tibial surface to create a 2 *mm* wide flat incision. Subsequently, a single 2 *mm* thick slice of tissue was cut parallel to the flat incision and was placed, on the sectioned side, on a specially constructed cutting die (Goertzen, 1992) to stamp out a dumbbell-shaped testing specimen with a 2 *mm* gauge width. In this manner, a total of 18 dumbbell-shaped circumferential-central specimens were harvested from 18 porcine lateral menisci ($n = 6$ per group). Each of these specimens was stored in a 50 mL tube with DMEM at 4 ℃ prior to tensile testing.

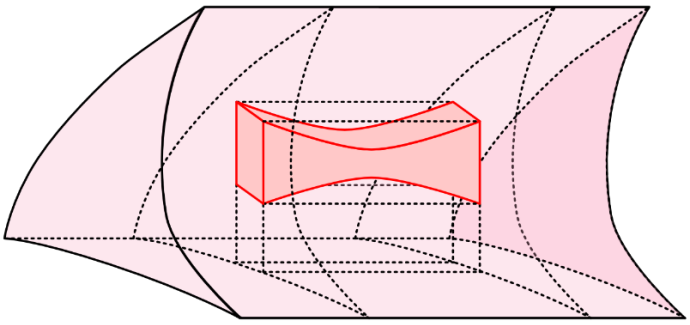

Figure 3-7: A Schematic Illustrating the Circumferential-Central Specimen

3.1.3.3 Longitudinal Orientation

Longitudinal specimens were harvested along the longitudinal orientation from the central region of each lateral meniscus (Figure 3-8). Initially, a thin slice was removed with a surgical blade oriented perpendicular to the peripheral edge to flatten the tibial surface. Subsequently, a single $2\ mm$ thick slice of tissue was cut parallel to the flat incision and was placed, on the sectioned side, on a specially constructed cutting die (Goertzen, 1992) to stamp out a dumbbell-shaped testing specimen with a 2 *mm* gauge width. The cutting die was aligned perpendicular to the radial fibers. In this manner, a total of 18 dumbbell-shaped longitudinal specimens were harvested from 18 porcine lateral menisci ($n = 6$ per group). Each of these specimens was stored in a $50\ mL$ tube with DMEM at 4 ℃ prior to tensile testing.

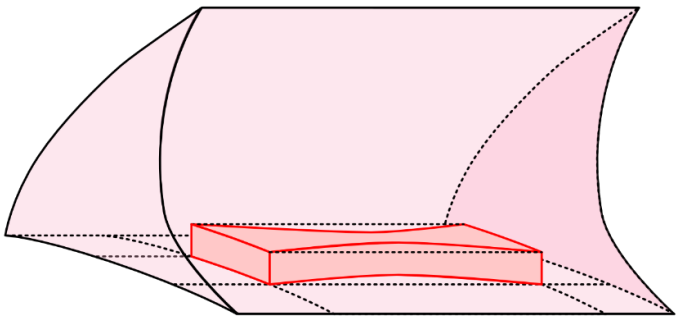

Figure 3-8: A Schematic Illustrating the Longitudinal Specimen

3.1.3.4 Radial Orientation

Radial specimens were harvested along the radial orientation from the central region of each lateral meniscus (Figure 3-9). Initially, a thin slice was removed with a surgical blade oriented perpendicular to the peripheral edge to flatten the tibial surface. Subsequently, a single $2\ mm$ thick slice of tissue was cut parallel to the flat incision and was placed, on the sectioned side, on a

specially constructed cutting die (Goertzen, 1992) to stamp out a dumbbell-shaped testing specimen with a 2 mm gauge width. The cutting die was aligned parallel to the radial fibers. In this manner, a total of 18 dumbbell-shaped radial specimens were harvested from 18 porcine lateral menisci ($n = 6$ per group). Each of these specimens was stored in a 50 mL tube with DMEM at 4 ℃ prior to tensile testing.

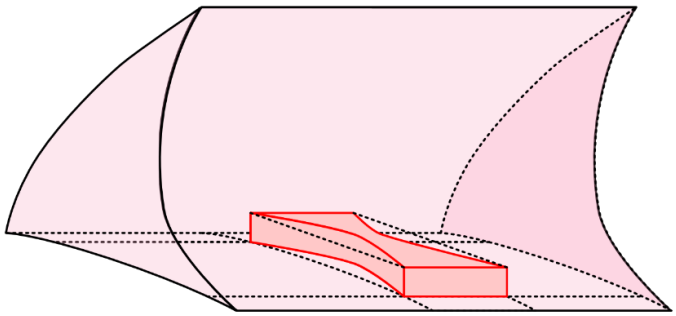

Figure 3-9: A Schematic Illustrating the Radial Specimen

3.1.4 Dimensional Measurements

3.1.4.1 Compression Specimens

Prior to compression testing, the dimensions of each cylindrical specimen were measured using a digital caliper with an accuracy of $\pm$ 0.01 mm. Initially, three equally spaced points were marked along the circular base of each cylindrical specimen. Subsequently, three repeated diameter and thickness measurements were made at each marked point and were used to calculate the average diameter and thickness of each cylindrical specimen.

3.1.4.2 Tensile Specimens

Prior to tensile testing, the dimensions of each dumbbell-shaped specimen were measured using a digital caliper with an accuracy of $\pm$ 0.01 mm. Initially, two parallel lines were marked 5 mm apart at each end of the narrow portion and the distance between the two parallel lines was designated as the gauge length. The gauge length of each tensile specimen was designed based on the preliminary experiments and literature review (Table 2-1). Three equally spaced locations were then marked along the gauge length of the dumbbell-shaped specimen. Subsequently, three repeated width and thickness measurements were made at each marked location and were used to calculate the average width and thickness of each dumbbell-shaped specimen.

3.2 Mechanical Testing

Cylindrical specimens were prepared for unconfined compressive stress-relaxation testing and dumbbell-shaped specimens were prepared for quasi-static tensile testing. Both the compressive and tensile testing were performed using Bose ElectroForce 3200 Series III test instrument (Figure 3-10) with a $\pm$225 N load cell (max error $\pm$0.27%) and a $\pm$6.5 mm displacement sensor (max error $\pm$0.14%). The load cell was attached to the micro-adjust shaft mounted on the movable lower crosshead. The lower extension shaft was attached to the load cell and the upper extension shaft was attached to the linear motor mounted on the stationary upper crosshead.

Figure 3-10: Bose ElectroForce 3200 Series III Test Instrument

3.2.1 Unconfined Compressive Stress-Relaxation Testing

The cylindrical specimen was immersed in a room temperature PBS bath (Figure 3-11) during unconfined compressive stress-relaxation testing. The PBS bath was secured to the movable lower crosshead and the lower extension shaft was attached to the load cell through the bottom of the bath. After a preload of $-1\ N$ was applied at a rate of $0.005\ N/sec$ and was held for 120 seconds, the stress-relaxation testing was performed. Each cylindrical specimen was compressed to 15% strain at a strain rate of $15\%/sec$. Then, the specimen was held at the 15% strain level and allowed to relax for 900 seconds. The amount of relaxation time was chosen on the basis of preliminary experiments to allow each compressed specimen to approach equilibrium.

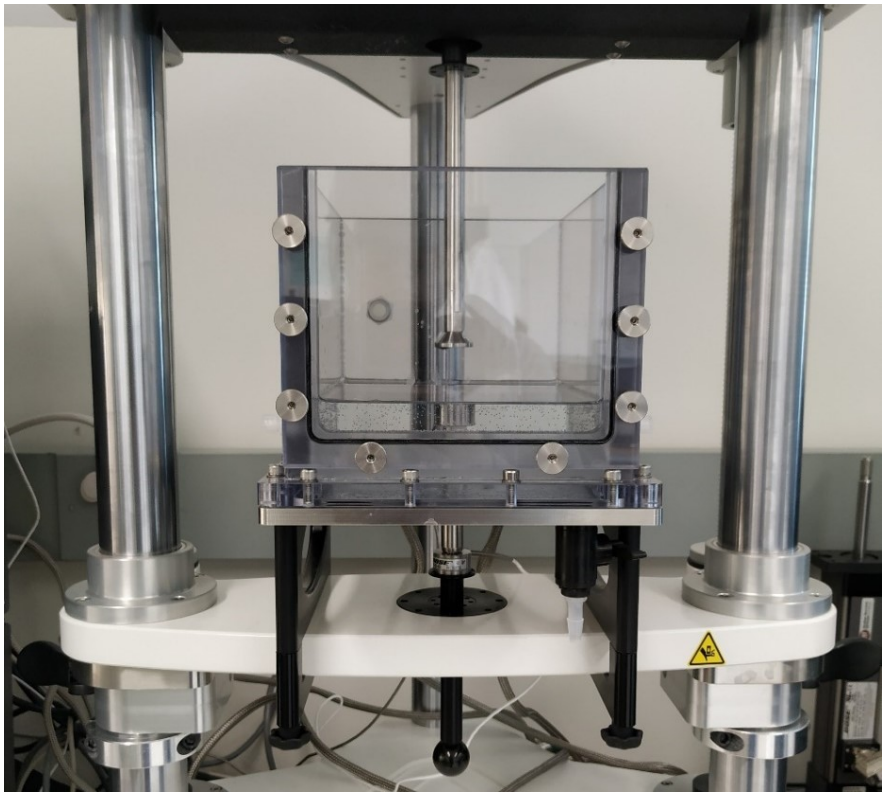

Figure 3-11: PBS Bath for Unconfined Compressive Stress-Relaxation Testing

3.2.2 Quasi-Static Tensile Testing

The dumbbell-shaped specimen was mounted between the two Bose grips (Figure 3-12) at each gauge line and each Bose grip was tightened to a rigid frame with an Allen wrench to minimize slippage. The top grip was attached to the upper extension shaft mounted on the stationary upper crosshead and the bottom grip was attached to the lower extension shaft mounted on the movable lower crosshead. Immediately after a preload of $0.2\ N$ was applied at $0.005\ N/sec$, each specimen was preconditioned cyclically to 3% strain at a displacement rate of $0.01\ mm/sec$ for 10 cycles. The cyclic preconditioning was achieved with a sinusoidal waveform at $0.033\ Hz$. Subsequently, the specimen was elongated to failure at a displacement rate of $0.01\ mm/sec$. This slow rate was chosen based on the loading protocols of previous studies (Table 2-1) to ensure a quasi-static testing condition by minimizing the flow-generated stiffening effect (Akizuki et al., 1986).

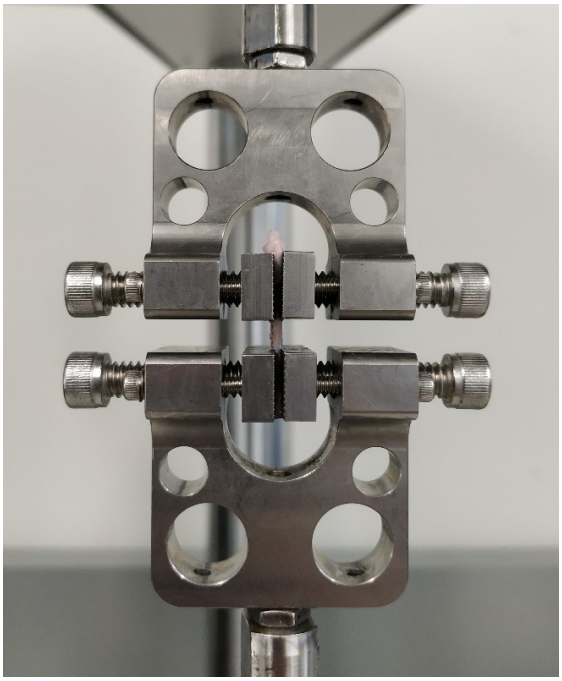

Figure 3-12: A Tensile Specimen Mounted Between Two Bose Grips

3.3 Data Analysis

3.3.1 Unconfined Compressive Stress-Relaxation Testing

For unconfined compressive stress-relaxation testing, the experimental results comprised of time, displacement, and load data were processed in Microsoft Excel 2016. A schematic of a typical stress-relaxation curve is shown in Figure 3-13. From the collected data, peak stress and secant modulus, instantaneous modulus, equilibrium stress and equilibrium modulus, and percent stress relaxation were determined. The strain was defined as the displacement divided by the initial thickness of each cylindrical specimen. The stress was calculated by dividing the measured load by the initial cross-sectional area. The peak stress was the maximum stress reached during the rapid loading, before the first decrease in load was detected. The secant modulus was defined as the peak stress divided by the applied strain (Andrews et al., 2015). The stress-strain response curve was constructed from the data of the rapid loading portion for each specimen and a linear regression model was utilized between 25% and 75% of peak stress to account for the nonlinear behavior in the initial region and the strain hardening region. The slope of that linear regression model was termed instantaneous modulus. The equilibrium stress was calculated by taking the average of the stresses from the last 30 data points of the stress-relaxation phase. For each of the last 30 data points, a modulus was calculated by dividing the stress by the corresponding strain. The equilibrium modulus was then calculated by taking the average of the moduli from the last 30 data points. The percent stress relaxation was calculated as the difference between the peak stress and the equilibrium stress divided by the peak stress.

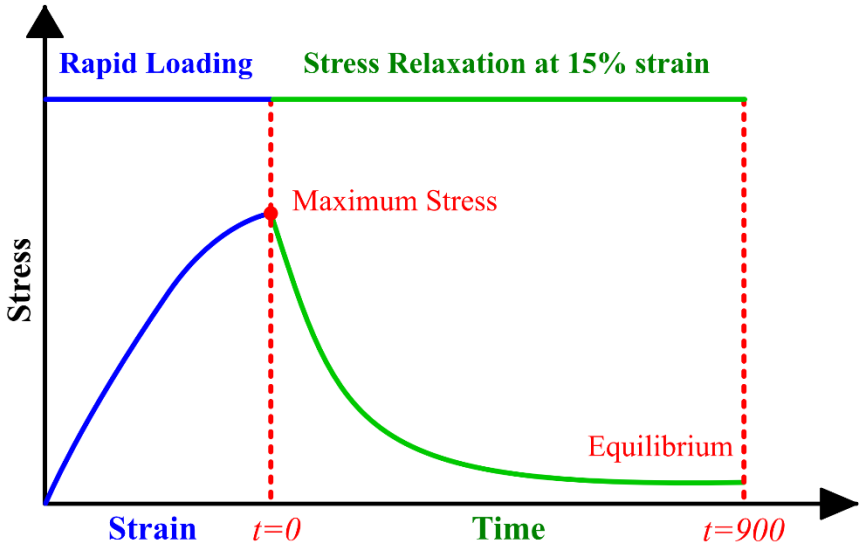

Figure 3-13: A Schematic of a Typical Stress-Relaxation Curve

Experimental results comprised of time and stress data were imported into MATLAB R2010a, and the stress-relaxation behavior of each specimen was modeled and characterized in MATLAB R2010a using the 3-term Prony series (Andrews et al., 2015) with customized codes written based on the least-squares algorithm. The behavior of the 3-term Prony series was governed by the following mathematical equation:

$$\sigma(t) = \sigma_\infty + \sum_{i=1}^{3} \sigma_i \cdot e^{(-t/\tau_i)}$$

where,

σ_∞ = equilibrium stress (MPa)

σ_i = Maxwell spring constants (MPa)

t = time (sec)

τ_i = relaxation time constants (sec)

The speed of stress-relaxation process is characterized in terms of relaxation time constants τ_i which is defined as the time needed for the stress to decrease to $1/e$ of the interval between Maxwell spring constants σ_i (Obaid et al., 2017). From the 3-term Prony series model, three relaxation time constants (τ_1, τ_2, τ_3) were determined for each specimen. The greater the values, the longer the time for the stress to relax, and thus the lower the permeability in the tissue.

3.3.2 Quasi-Static Tensile Testing

For quasi-static tensile testing, failure was considered to occur when the dumbbell-shaped specimen broke in half (Figure 3-14) or the first decrease in load was detected. The experimental results comprised of load and displacement data were processed and analyzed in Microsoft Excel 2016. A schematic of a typical stress-strain response curve is shown in Figure 3-15. From the collected data, ultimate tensile stress, failure strain, and tensile modulus were determined. The strain was defined as the displacement divided by the initial gauge length of each dumbbell-shaped specimen. The stress was calculated by dividing the measured load by the initial cross-sectional area, which was the multiplication of the average width by the average thickness for the gauge section. The ultimate tensile stress was taken as the maximum stress achieved during the tensile testing and the strain at ultimate tensile stress was referred to as the failure strain. The stress-strain response curve was constructed for each specimen and a linear regression model was utilized

between 25% and 75% of maximum stress. The slope of that linear regression was taken as an estimate of the tensile modulus.

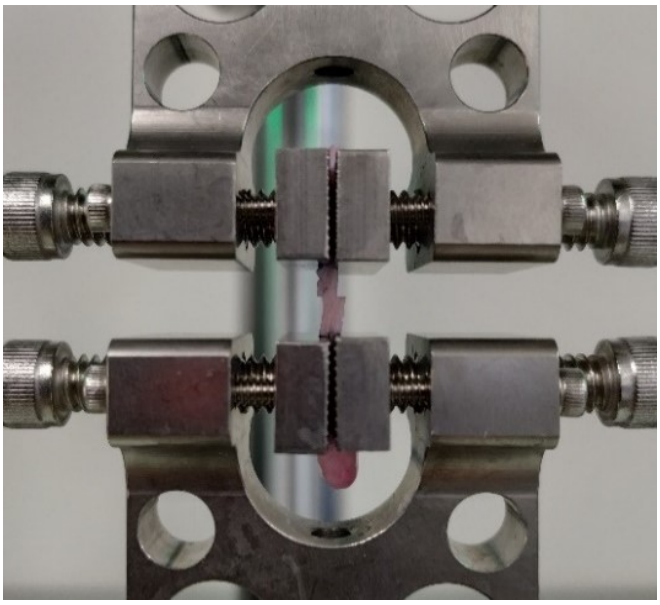

Figure 3-14: Failure of a Tensile Specimen

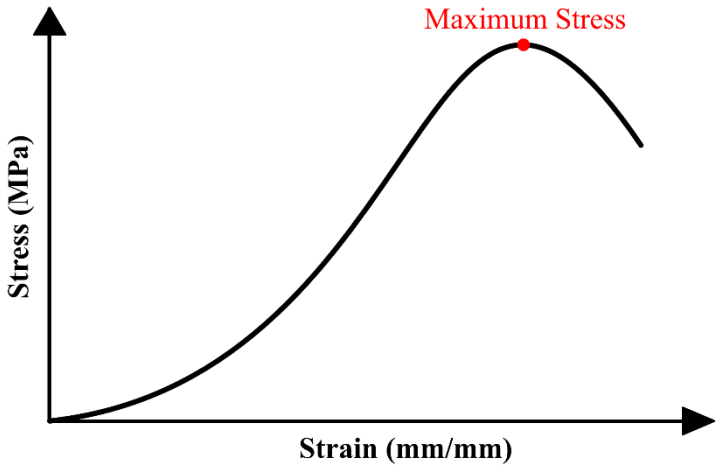

Figure 3-15: A Schematic of a Typical Stress-Strain Response Curve

3.4 Statistical Analysis

Descriptive statistics including the mean and standard deviation were calculated with Microsoft Excel 2016 built-in functions. To test the primary hypothesis that the fresh and vitrified menisci would exhibit comparable mechanical properties whereas frozen menisci would exhibit inferior mechanical properties, one-way analysis of variance (ANOVA) with linear contrasts was performed in Microsoft Excel 2016 for each mechanical parameter to evaluate the statistical significance and a p-value < 0.05 was accepted as significant. For each mechanical parameter, linear contracts allow three group-wise comparisons, namely fresh vs. frozen, fresh vs. vitrified, and frozen vs. vitrified. Furthermore, to test the secondary hypothesis that specimens along the circumferential-peripheral orientation would exhibit superior tensile mechanical properties while specimens along the radial orientation would exhibit inferior tensile mechanical properties, ANOVA with linear contrasts was performed in Microsoft Excel 2016 for each mechanical parameter to evaluate the statistical significance and a p-value < 0.05 was accepted as significant. For each mechanical parameter, linear contracts allow five group-wise comparisons, namely circumferential-peripheral vs. circumferential-central, circumferential-peripheral vs. longitudinal, circumferential-peripheral vs. radial, circumferential-central vs. radial, longitudinal vs. radial.

3.4.1 Outliers

Outliers were identified with Microsoft Excel 2016 boxplot. The boxplot (Figure 3-16) is a schematic presentation of the minimum, first quartile, median, third quartile, and maximum (Hayter, 2013). In a typical boxplot, the rectangular box spans the first quartile to the third quartile with a horizontal segment drawn in the middle to represent the median. There are two “whiskers”

drawn above and below the box indicating the locations of the minimum and maximum of the dataset. The minimum and maximum refer to the smallest or largest data point excluding any outliers, respectively. The median is the middle value of the dataset. The first quartile is the middle value between the smallest data and the median, whereas the third quartile is the middle value between the median and the largest data. The interquartile range (IQR) refers to the distance between the first quartile and the third quartile. A data point is considered as an outlier if it exceeds a distance of either 1.5 times the IQR above the third quartile or 1.5 times the IQR below the first quartile. The identified outliers were removed from the dataset and statistical analysis was performed without the outliers.

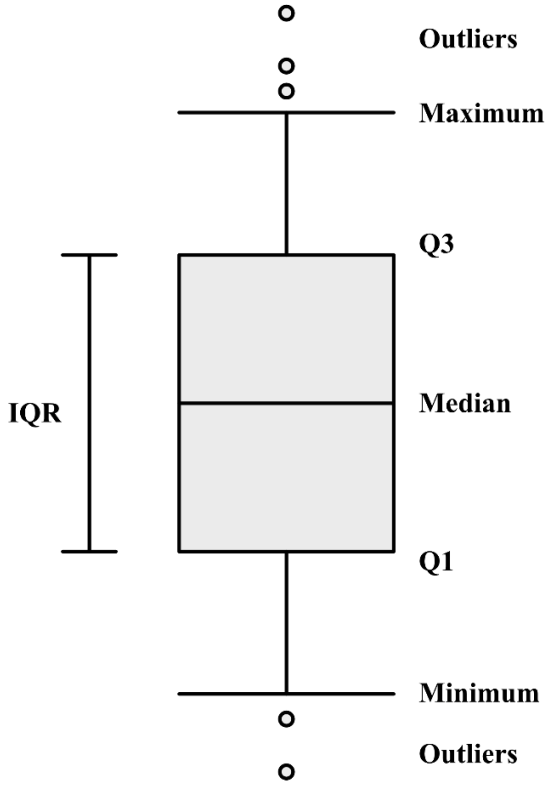

Figure 3-16: A Schematic Illustrating the Boxplot

Chapter 4: Results

4.1 Unconfined Compressive Stress-Relaxation Testing

4.1.1 Compressive Mechanical Properties

Compressive mechanical properties including the peak stress (MPa) and secant modulus (MPa), equilibrium stress (MPa) and equilibrium modulus (MPa), instantaneous modulus (MPa), and percent stress relaxation (%) were determined and tabulated in Appendix A for each group. Outliers in each group were identified with the boxplot (Appendix B) and were excluded from the analysis (two samples in each of the fresh and frozen groups, and three samples in the vitrified group). The mean and standard deviation (SD) values of the compressive mechanical properties for fresh, frozen, and vitrified groups ($n = 10$ in the fresh and frozen groups, $n = 9$ in the vitrified group) are presented in Table 4-1. ANOVA with linear contrasts was performed for the secant modulus, equilibrium modulus, and instantaneous modulus between the groups. In summary, the compressive mechanical properties of vitrified menisci were comparable to that of fresh menisci, whereas frozen menisci exhibited inferior compressive mechanical properties.

Table 4-1: Mean and Standard Deviation of Compressive Mechanical Properties

Test Group	Descriptive Statistics	Peak Stress (MPa)	Secant Modulus (MPa)	Equilibrium Stress (MPa)	Equilibrium Modulus (MPa)	Instantaneous Modulus (MPa)	Percent Relaxation (%)
Fresh	Mean	-4.7	31.5	-0.03	0.19	47.9	99.4
	SD	0.5	3.2	0.01	0.09	4.7	0.2
Frozen	Mean	-3.2	21.1	-0.02	0.12	32.1	99.4
	SD	0.9	6.1	0.01	0.05	8.8	0.3
Vitrified	Mean	-4.4	29.1	-0.03	0.17	43.5	99.4
	SD	0.6	3.8	0.01	0.04	5.6	0.2

4.1.1.1 Secant Modulus

The mean secant modulus of vitrified menisci ($29.1 \pm 3.8\ MPa$) was comparable to that of fresh menisci ($31.5 \pm 3.2\ MPa$). However, the mean secant modulus of frozen menisci ($21.1 \pm 6.1\ MPa$) was significantly lower than that of fresh menisci ($p < 0.001$) and vitrified menisci ($p < 0.001$). The boxplot of the secant modulus is shown in Figure 4-1.

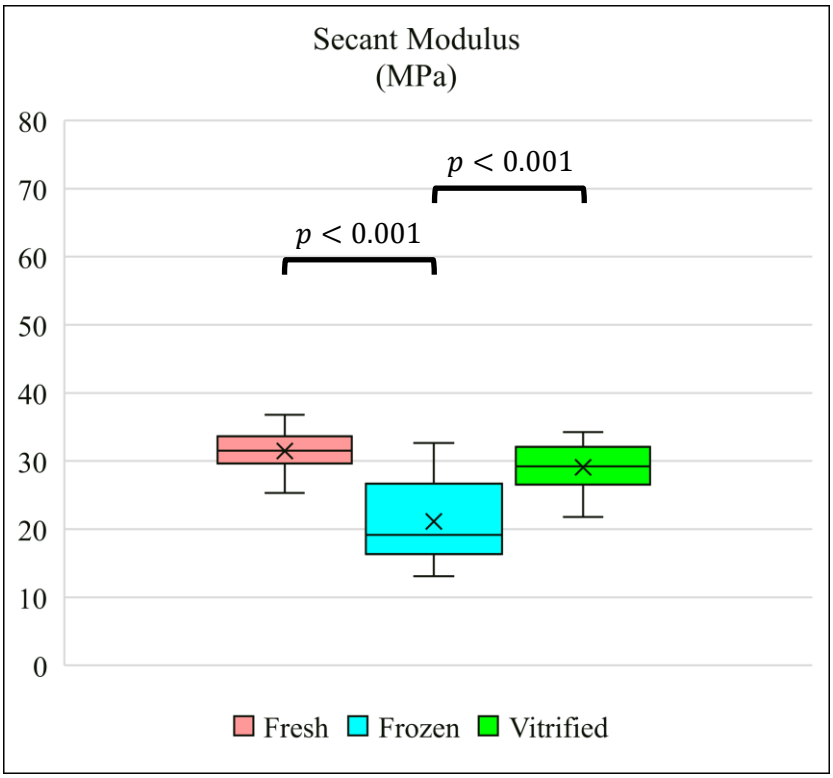

Figure 4-1: Boxplot – Secant Modulus

4.1.1.2 Equilibrium Modulus

The mean equilibrium modulus of vitrified menisci ($0.17 \pm 0.04\ MPa$) was comparable to that of fresh menisci ($0.19 \pm 0.09\ MPa$). By comparison, the mean equilibrium modulus of frozen menisci ($0.12 \pm 0.05\ MPa$) was significantly lower than that of fresh menisci ($p = 0.038$). The boxplot of the equilibrium modulus is shown in Figure 4-2.

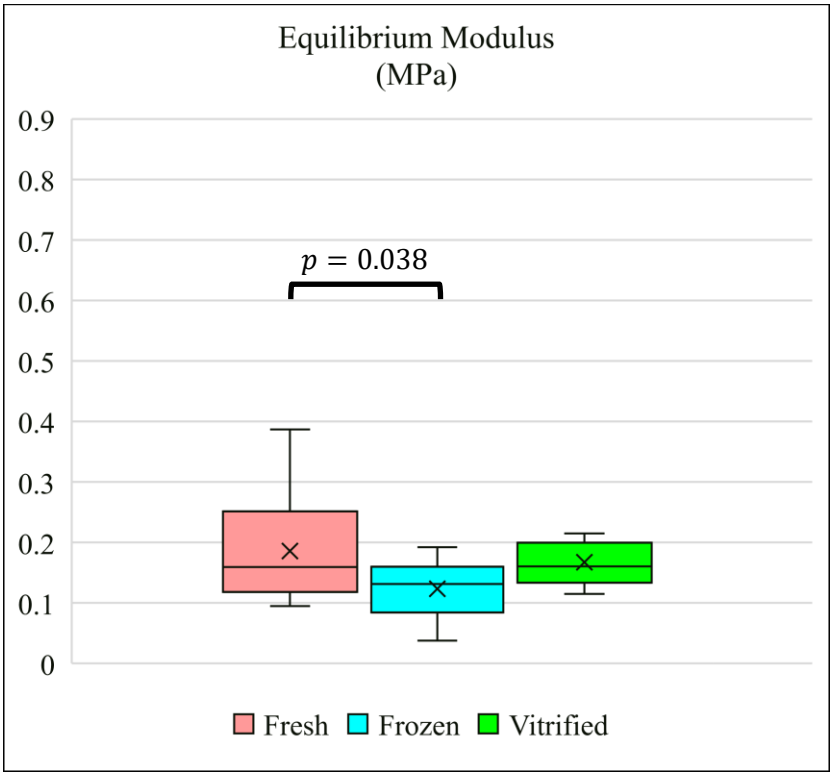

Figure 4-2: Boxplot – Equilibrium Modulus

4.1.1.3 Instantaneous Modulus

The mean instantaneous modulus of vitrified menisci ($43.5 \pm 5.6\ MPa$) was comparable to that of fresh menisci ($47.9 \pm 4.7\ MPa$). However, the mean instantaneous modulus of frozen menisci ($32.1 \pm 8.8\ MPa$) was significantly lower than that of fresh menisci ($p < 0.001$) and vitrified menisci ($p < 0.001$). The boxplot of the instantaneous modulus is shown in Figure 4-3.

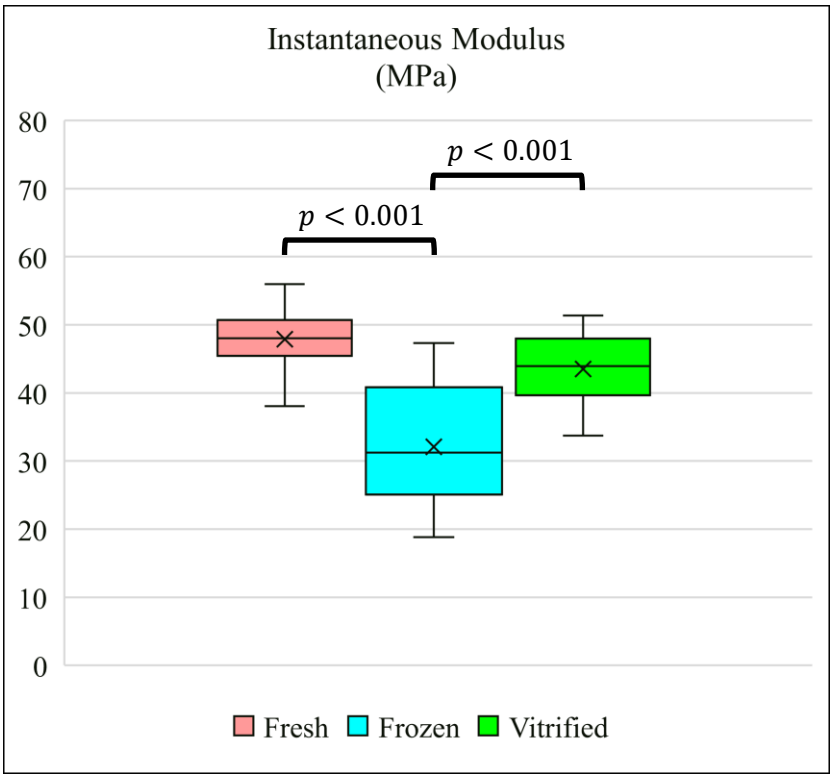

Figure 4-3: Boxplot – Instantaneous Modulus

4.1.2 Three-Term Prony Series

From the 3-term Prony series model, three relaxation time constants (τ_1, τ_2, τ_3) of each specimen were determined and tabulated in Appendix A for each group. Outliers in each group were identified with the boxplot (Appendix B) and were excluded from the analysis. The mean and standard deviation (SD) values of each relaxation time constant for fresh, frozen, and vitrified groups are presented in Table 4-2.

Table 4-2: Mean and Standard Deviation of Three Relaxation Time Constants

Test Group	Descriptive Statistics	τ_1 (s)	τ_2 (s)	τ_3 (s)
Fresh	Mean	3.3	18.2	119.0
	SD	0.7	3.1	12.8
Frozen	Mean	2.8	16.7	113.8
	SD	0.6	3.6	16.0
Vitrified	Mean	3.1	17.4	113.3
	SD	0.4	1.5	8.5

ANOVA with linear contrasts was performed for each relaxation time constant between the groups. In summary, no statistical differences were detected in each relaxation time constant comparing the three groups. Specifically, the mean τ_1 of frozen menisci ($2.8 \pm 0.6\, MPa$) and vitrified menisci ($3.1 \pm 0.4\, MPa$) were comparable to that of fresh menisci ($3.3 \pm 0.7\, MPa$). Similarly, the mean τ_2 of frozen menisci ($16.7 \pm 3.6\, MPa$) and vitrified menisci ($17.4 \pm 1.5\, MPa$) were comparable to that of fresh menisci ($18.2 \pm 3.1\, MPa$). Likewise, the mean τ_3 of frozen menisci ($113.8 \pm 16.0\, MPa$) and vitrified menisci ($113.3 \pm 8.5\, MPa$) were comparable to that of fresh menisci ($119.0 \pm 12.8\, MPa$).

4.2 Quasi-Static Tensile Testing

4.2.1 Tensile Mechanical Properties along Circumferential-Peripheral Orientation

Tensile mechanical properties along the circumferential-peripheral orientation including the ultimate tensile stress (MPa), failure strain (mm/mm), and tensile modulus (MPa) were determined and tabulated in Appendix A for each group. The mean and standard deviation (SD) values of the tensile mechanical properties along the circumferential-peripheral orientation for fresh, frozen, and vitrified groups ($n = 6$ per group) are presented in Table 4-3. ANOVA with linear contrasts was performed for the ultimate tensile stress, failure strain, and tensile modulus between the groups.

Table 4-3: Mean and Standard Deviation of Tensile Mechanical Properties along Circumferential-Peripheral Orientation

Test Group	Descriptive Statistics	Ultimate Tensile Stress (MPa)	Failure Strain (mm/mm)	Tensile Modulus (MPa)
Fresh	Mean	41.2	0.62	97.9
	SD	8.0	0.10	25.0
Frozen	Mean	28.0	0.55	78.4
	SD	5.1	0.09	15.9
Vitrified	Mean	38.8	0.55	102.5
	SD	7.2	0.08	26.6

4.2.1.1 Ultimate Tensile Stress

The mean ultimate tensile stress along the circumferential-peripheral orientation of vitrified menisci ($38.8 \pm 7.2\ MPa$) was comparable to that of fresh menisci ($41.2 \pm 8.0\ MPa$). However, the mean ultimate tensile stress of frozen menisci ($28.0 \pm 5.1\ MPa$) was significantly lower than that of fresh menisci ($p = 0.005$) and vitrified menisci ($p = 0.016$). The boxplot of the ultimate tensile stress (MPa) along the circumferential-peripheral orientation is shown in Figure 4-4.

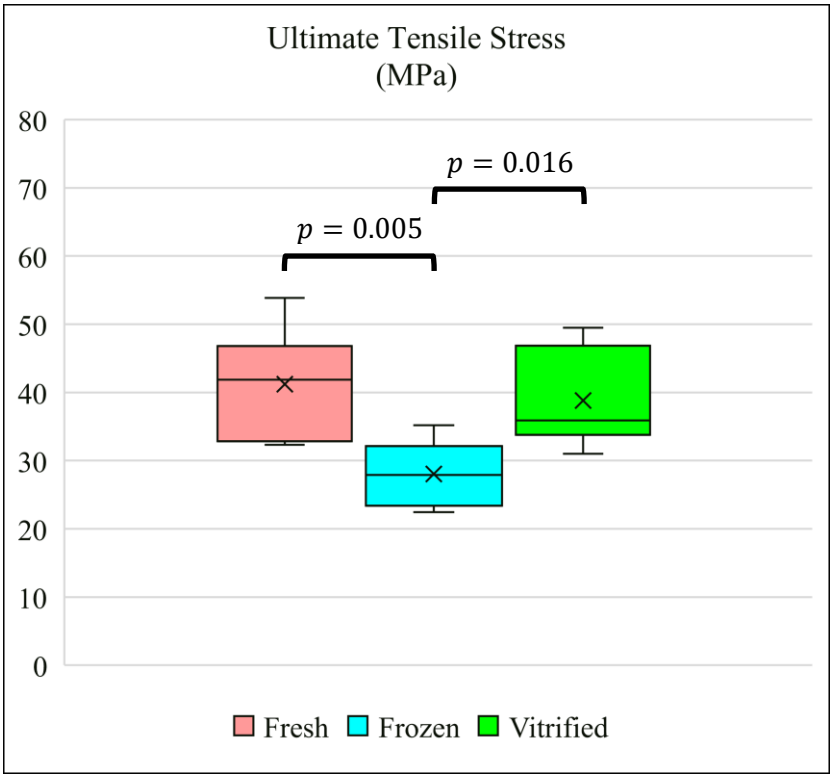

Figure 4-4: Boxplot – Circumferential-Peripheral Orientation – Ultimate Tensile Stress

4.2.1.2 Failure Strain

No statistical differences were detected in the failure strain along the circumferential-peripheral orientation comparing the three groups. Specifically, the mean failure strain of vitrified menisci ($0.55 \pm 0.08\, mm/mm$) and frozen menisci ($0.55 \pm 0.09\, mm/mm$) were comparable to that of fresh menisci ($0.62 \pm 0.10\, mm/mm$). The boxplot of the failure strain (mm/mm) along the circumferential-peripheral orientation is shown in Figure 4-5.

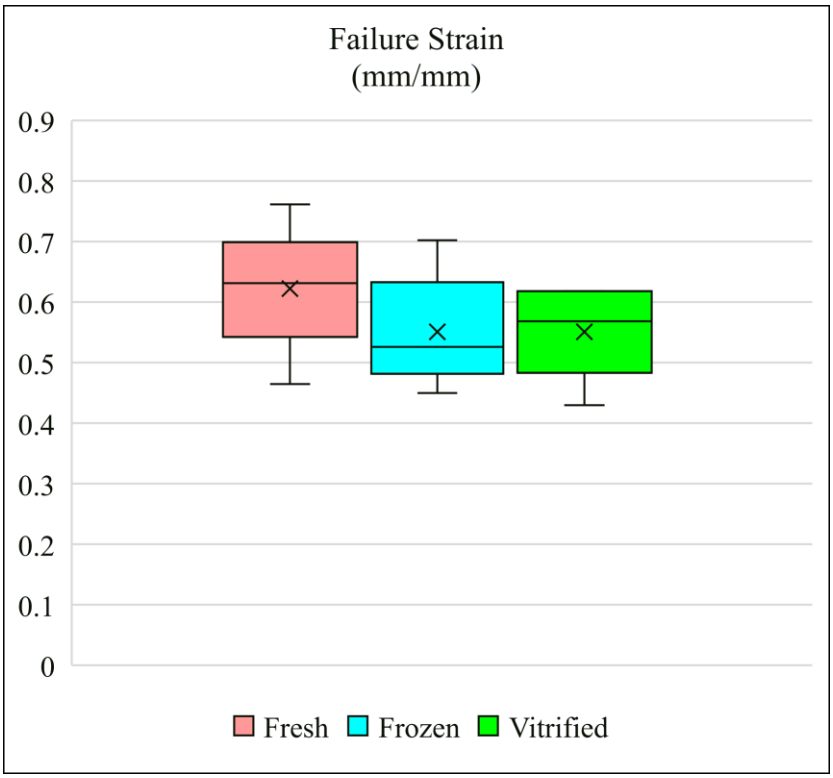

Figure 4-5: Boxplot – Circumferential-Peripheral Orientation – Failure Strain

4.2.1.3 Tensile Modulus

No statistical differences were detected in the tensile modulus along the circumferential-peripheral orientation comparing the three groups. Specifically, the mean tensile modulus of vitrified menisci $(102.5 \pm 26.6\ MPa)$ was comparable to that of fresh menisci $(97.9 \pm 25.0\ MPa)$ while the mean tensile modulus of frozen menisci was $78.4 \pm 15.9\ MPa$. The boxplot of the tensile modulus (MPa) along the circumferential-peripheral orientation is shown in Figure 4-6.

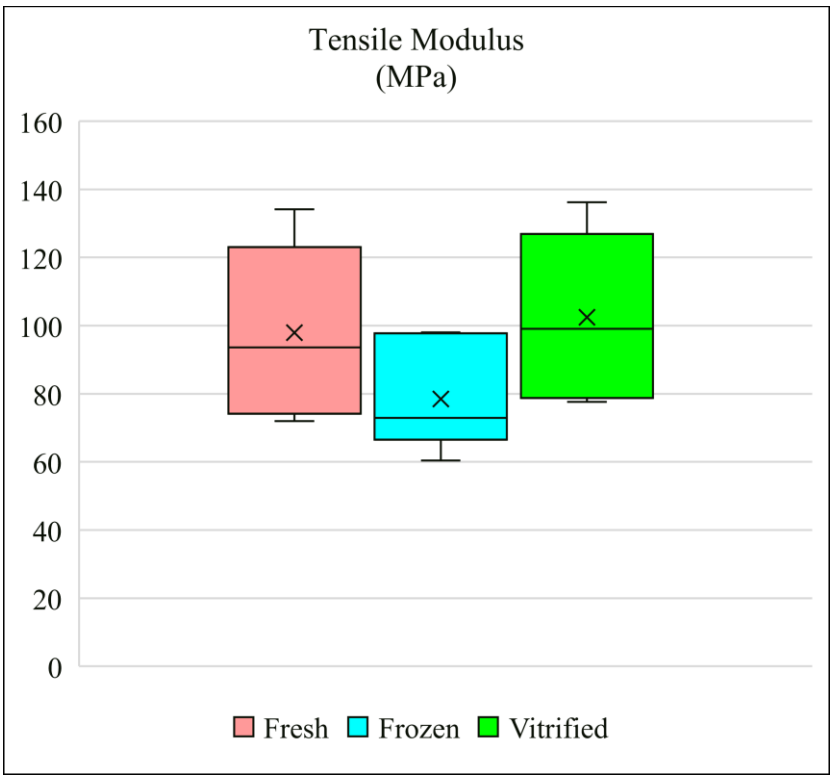

Figure 4-6: Boxplot – Circumferential-Peripheral Orientation – Tensile Modulus

4.2.2 Tensile Mechanical Properties along Circumferential-Central Orientation

Tensile mechanical properties along the circumferential-central orientation including the ultimate tensile stress (MPa), failure strain (mm/mm), and tensile modulus (MPa) were determined and tabulated in Appendix A. The mean and standard deviation (SD) values of the tensile mechanical properties along the circumferential-central orientation for fresh, frozen, and vitrified groups ($n = 6$ per group) are presented in Table 4-4. ANOVA with linear contrasts was performed for the ultimate tensile stress, failure strain, and tensile modulus between the groups.

Table 4-4: Mean and Standard Deviation of Tensile Mechanical Properties along Circumferential-Central Orientation

Test Group	Descriptive Statistics	Ultimate Tensile Stress (MPa)	Failure Strain (mm/mm)	Tensile Modulus (MPa)
Fresh	Mean	26.0	0.42	95.0
	SD	5.9	0.08	8.2
Frozen	Mean	22.9	0.43	74.1
	SD	2.8	0.08	8.0
Vitrified	Mean	26.5	0.46	87.0
	SD	4.2	0.08	22.1

4.2.2.1 Ultimate Tensile Stress

No statistical differences were detected in the ultimate tensile stress along the circumferential-central orientation comparing the three groups. Specifically, the mean ultimate tensile stress of vitrified menisci ($26.5 \pm 4.2\ MPa$) was comparable to that of fresh menisci ($26.0 \pm 5.9\ MPa$) while the mean ultimate tensile stress of frozen menisci was $22.9 \pm 2.8\ MPa$. The boxplot of the ultimate tensile stress (MPa) along the circumferential-central orientation is shown in Figure 4-7.

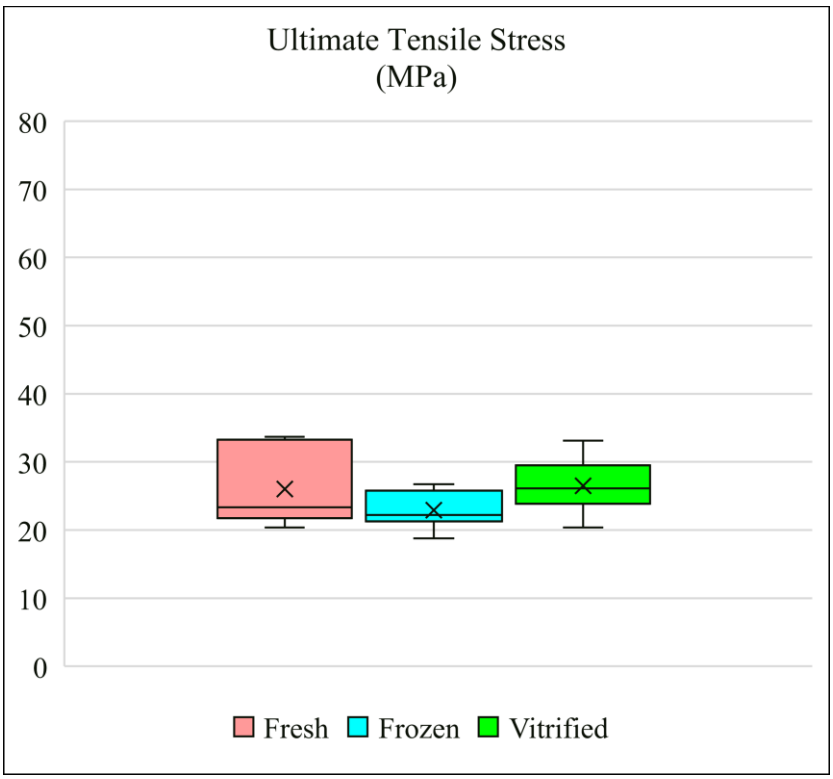

Figure 4-7: Boxplot – Circumferential-Central Orientation – Ultimate Tensile Stress

4.2.2.2 Failure Strain

No statistical differences were detected in the failure strain along the circumferential-central orientation comparing the three groups. Specifically, the mean failure strain of vitrified menisci $(0.46 \pm 0.08\, MPa)$ and frozen menisci $(0.43 \pm 0.08\, MPa)$ were comparable to that of fresh menisci $(0.42 \pm 0.08\, MPa)$. The boxplot of the failure strain (mm/mm) along the circumferential-central orientation is shown in Figure 4-8.

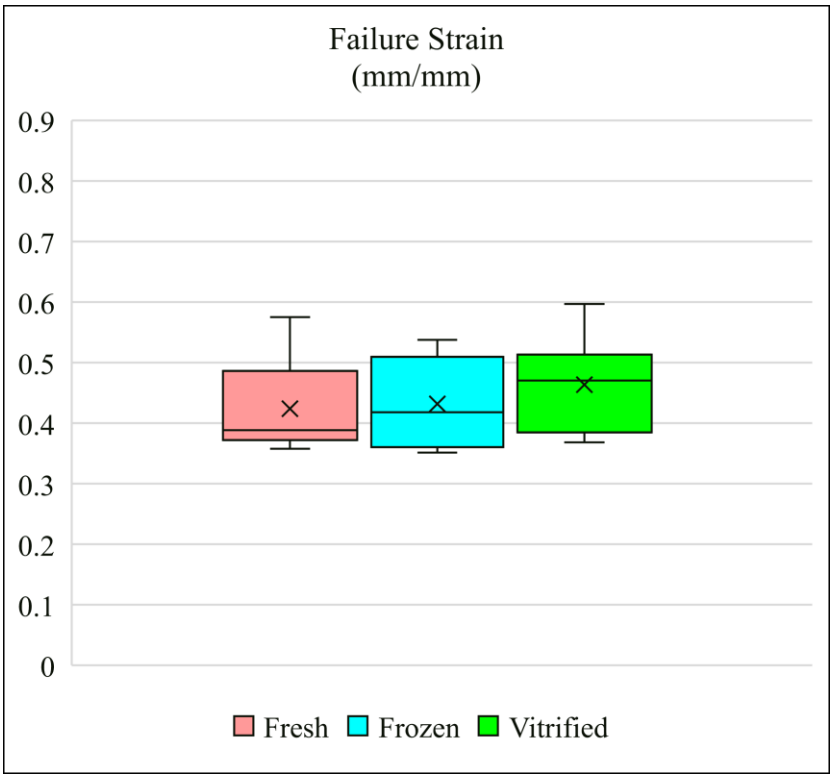

Figure 4-8: Boxplot – Circumferential-Central Orientation – Failure Strain

4.2.2.3 Tensile Modulus

The mean tensile modulus along the circumferential-central orientation of vitrified menisci ($87.0 \pm 22.1\ MPa$) was comparable to that of fresh menisci ($95.0 \pm 8.2\ MPa$). By comparison, the mean tensile modulus of frozen menisci ($74.1 \pm 8.0\ MPa$) was significantly lower than that of fresh menisci ($p = 0.024$). The boxplot of the tensile modulus (MPa) along the circumferential-central orientation is shown in Figure 4-9.

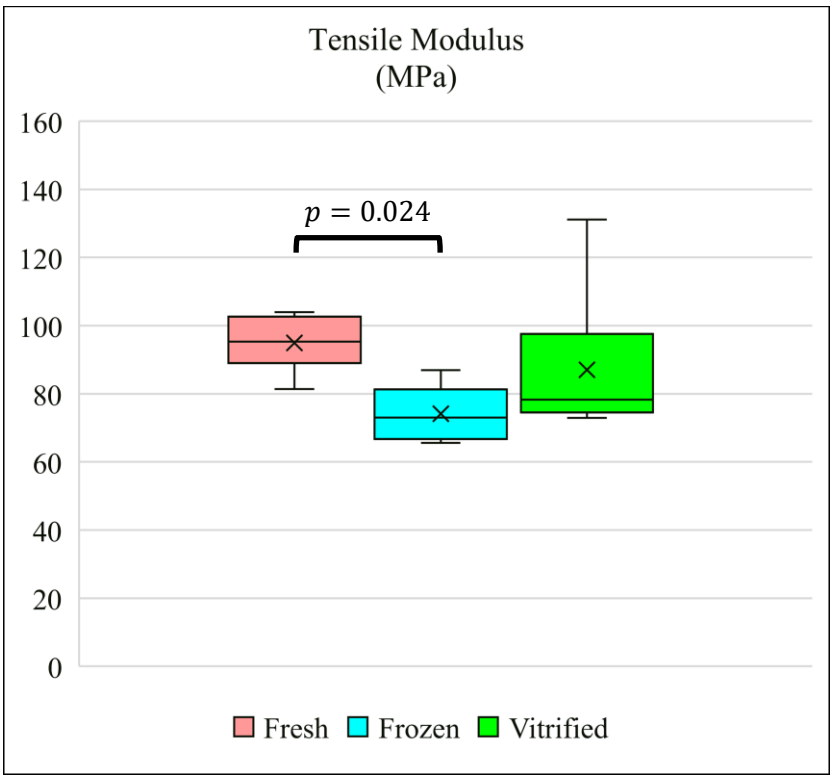

Figure 4-9: Boxplot – Circumferential-Central Orientation – Tensile Modulus

4.2.3 Tensile Mechanical Properties along Longitudinal Orientation

Tensile mechanical properties along the longitudinal orientation including the ultimate tensile stress (MPa), failure strain (mm/mm), and tensile modulus (MPa) were determined and tabulated in Appendix A for each group. One sample in the frozen group was identified as an outlier with the boxplot. Although the outlier was not excluded from the analysis owing to the small sample size of each group, the effect of excluding the outlier are presented in Appendix B and was reported in the following subsections. The mean and standard deviation (SD) values of the tensile mechanical properties along the longitudinal orientation for fresh, frozen, and vitrified groups ($n = 6$ per group) are presented in Table 4-5. ANOVA with linear contrasts was performed for the ultimate tensile stress, failure strain, and tensile modulus between the groups.

Table 4-5: Mean and Standard Deviation of Tensile Mechanical Properties along Longitudinal Orientation

Test Group	Descriptive Statistics	Ultimate Tensile Stress (MPa)	Failure Strain (mm/mm)	Tensile Modulus (MPa)
Fresh	Mean	28.3	0.41	98.9
	SD	4.6	0.06	4.2
Frozen	Mean	21.0	0.33	88.9
	SD	2.6	0.02	15.0
Vitrified	Mean	26.2	0.37	105.5
	SD	3.6	0.04	11.0

4.2.3.1 Ultimate Tensile Stress

The mean ultimate tensile stress along the longitudinal orientation of vitrified menisci $(26.2 \pm 3.6\ MPa)$ was comparable to that of fresh menisci $(28.3 \pm 4.6\ MPa)$. However, the mean ultimate tensile stress of frozen menisci $(21.0 \pm 2.6\ MPa)$ was significantly lower than that of fresh menisci $(p = 0.004)$ and vitrified menisci $(p = 0.029)$. The boxplot of the ultimate tensile stress (MPa) along the longitudinal orientation is shown in Figure 4-10.

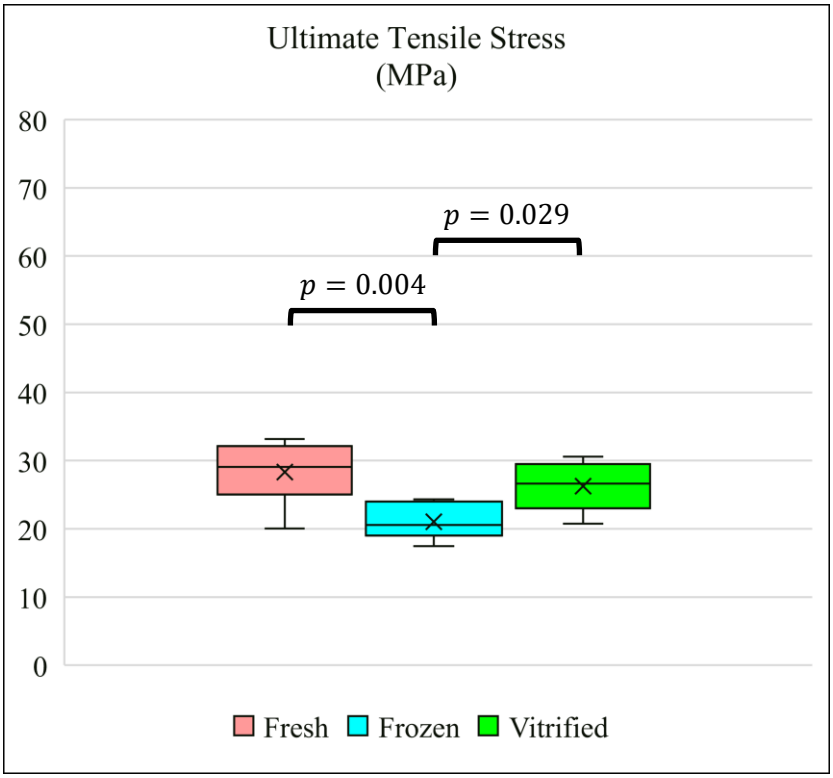

Figure 4-10: Boxplot – Longitudinal Orientation – Ultimate Tensile Stress

Excluding the outlier in the frozen group, the mean ultimate tensile stress along the longitudinal orientation of frozen menisci $(21.8 \pm 2.2\ MPa)$ was significantly lower than that of fresh menisci $(p = 0.011)$.

4.2.3.2 Failure Strain

The mean failure strain along the longitudinal orientation of vitrified menisci ($0.37 \pm 0.04\ MPa$) was comparable to that of fresh menisci ($0.41 \pm 0.06\ MPa$). However, the mean failure strain of frozen menisci ($0.33 \pm 0.02\ MPa$) was significantly lower than that of fresh menisci ($p = 0.012$). The boxplot of the failure strain (mm/mm) along the longitudinal orientation is shown in Figure 4-11.

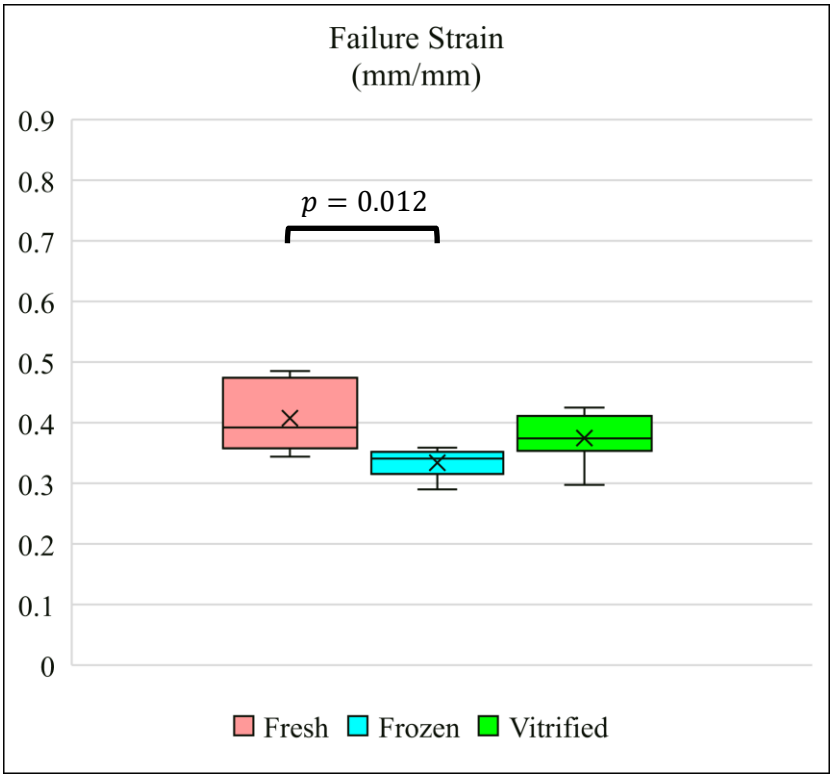

Figure 4-11: Boxplot – Longitudinal Orientation – Failure Strain

Excluding the outlier in the frozen group, the mean failure strain along the longitudinal orientation of frozen menisci ($0.33 \pm 0.02\ MPa$) was significantly lower than that of fresh menisci ($p = 0.013$).

4.2.3.3 Tensile Modulus

The mean tensile modulus along the longitudinal orientation of vitrified menisci ($105.5 \pm 11.0\ MPa$) was comparable to that of fresh menisci ($98.9 \pm 4.2\ MPa$). By comparison, the mean tensile modulus of frozen menisci ($88.9 \pm 15.0\ MPa$) was significantly lower than that of vitrified menisci ($p = 0.019$). The boxplot of the tensile modulus (MPa) along the longitudinal orientation is shown in Figure 4-12.

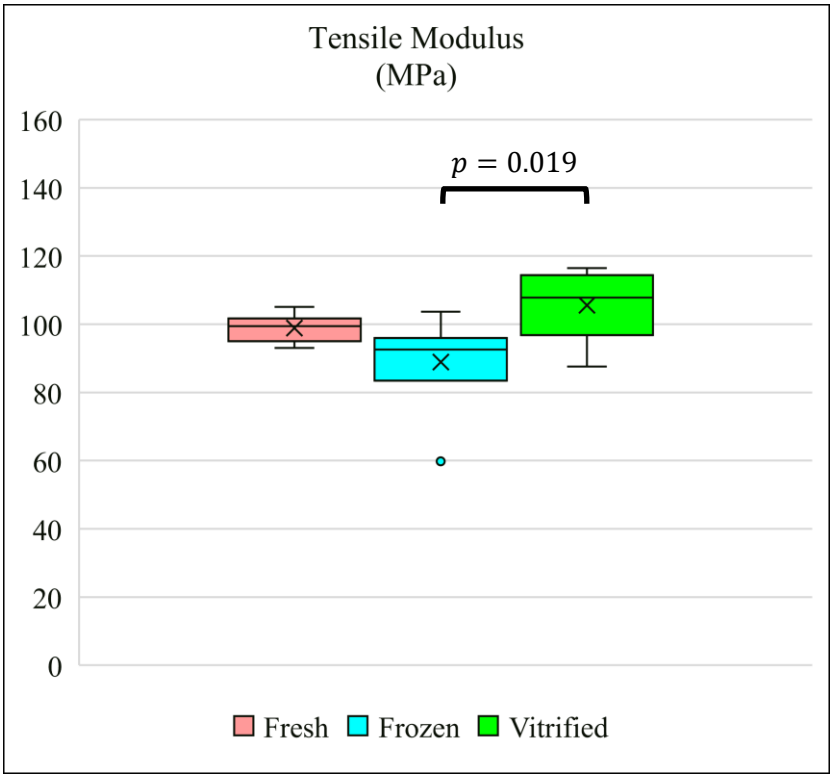

Figure 4-12: Boxplot – Longitudinal Orientation – Tensile Modulus

Excluding the outlier in the frozen group, the mean tensile modulus along the longitudinal orientation of frozen menisci ($94.7 \pm 5.1\ MPa$) was significantly lower than that of vitrified menisci ($p = 0.032$).

4.2.4 Tensile Mechanical Properties along Radial Orientation

Tensile mechanical properties along the radial orientation including the ultimate tensile stress (MPa), failure strain (mm/mm), and tensile modulus (MPa) were determined and tabulated in Appendix A for each group. The mean and standard deviation (SD) values of the tensile mechanical properties along the radial orientation for fresh, frozen, and vitrified groups ($n = 6$ per group) are presented in Table 4-6. ANOVA with linear contrasts was performed for the ultimate tensile stress, failure strain, and tensile modulus between the groups.

Table 4-6: Mean and Standard Deviation of Tensile Mechanical Properties along Radial Orientation

Test Group	Descriptive Statistics	Ultimate Tensile Stress (MPa)	Failure Strain (mm/mm)	Tensile Modulus (MPa)
Fresh	Mean	11.7	0.42	42.5
	SD	2.1	0.06	7.4
Frozen	Mean	6.7	0.38	24.9
	SD	1.2	0.09	4.8
Vitrified	Mean	12.7	0.37	50.6
	SD	4.5	0.04	20.3

4.2.4.1 Ultimate Tensile Stress

The mean ultimate tensile stress along the radial orientation of vitrified menisci ($12.7 \pm 4.5\ MPa$) was comparable to that of fresh menisci ($11.7 \pm 2.1\ MPa$). However, the mean ultimate tensile stress of frozen menisci ($6.7 \pm 1.2\ MPa$) was significantly lower than that of fresh menisci ($p = 0.010$) and vitrified menisci ($p = 0.003$). The boxplot of the ultimate tensile stress (MPa) along the radial orientation is shown in Figure 4-13.

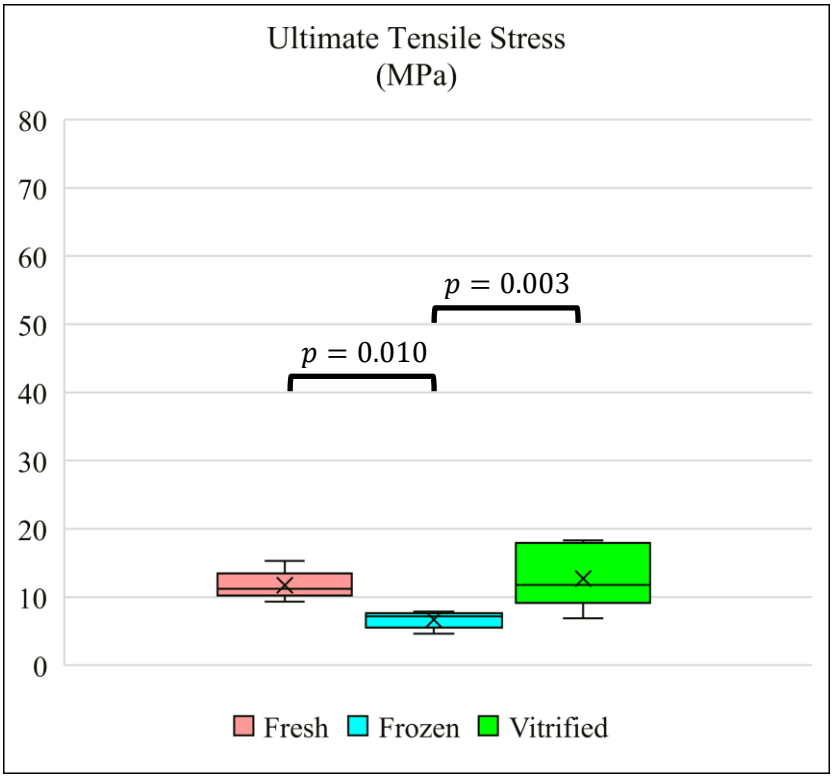

Figure 4-13: Boxplot – Radial Orientation – Ultimate Tensile Stress

4.2.4.2 Failure Strain

No statistical differences were detected in the failure strain along the radial orientation comparing the three groups. Specifically, the mean failure strain of vitrified menisci $(0.37 \pm 0.04\ MPa)$ and frozen menisci $(0.38 \pm 0.09\ MPa)$ were comparable to that of fresh menisci $(0.42 \pm 0.06\ MPa)$. The boxplot of failure strain (mm/mm) along the radial orientation is shown in Figure 4-14.

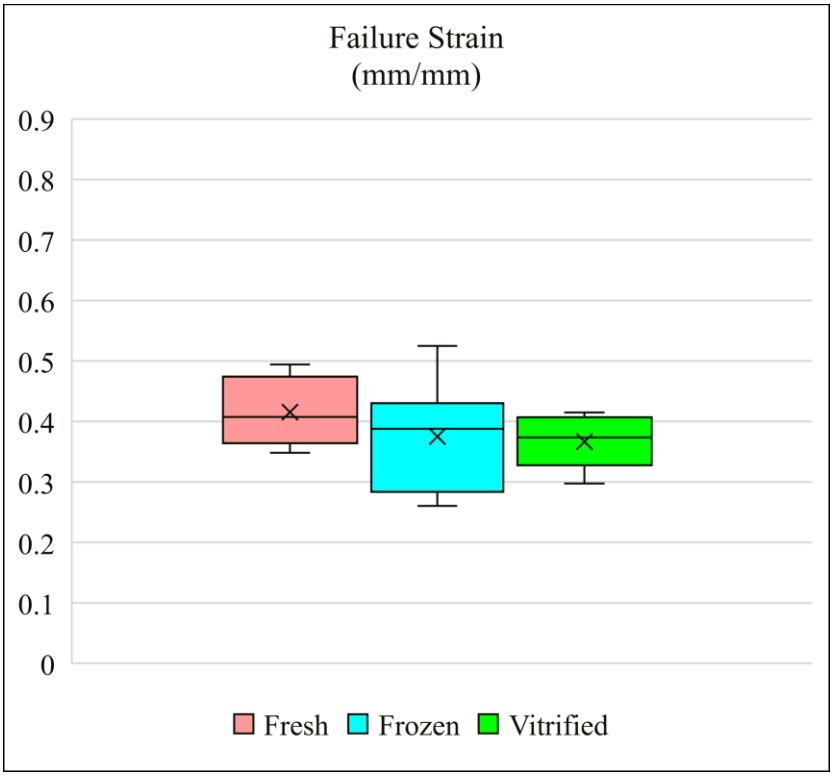

Figure 4-14: Boxplot – Radial Orientation – Failure Strain

4.2.4.3 Tensile Modulus

The mean tensile modulus along the radial orientation of vitrified menisci ($50.6 \pm 20.3\ MPa$) was comparable to that of fresh menisci ($42.5 \pm 7.4\ MPa$). By comparison, the mean tensile modulus of frozen menisci ($24.9 \pm 4.8\ MPa$) was significantly lower than that of fresh menisci ($p = 0.031$) and vitrified menisci ($p = 0.003$). The boxplot of the tensile modulus (MPa) along the radial orientation is shown in Figure 4-15.

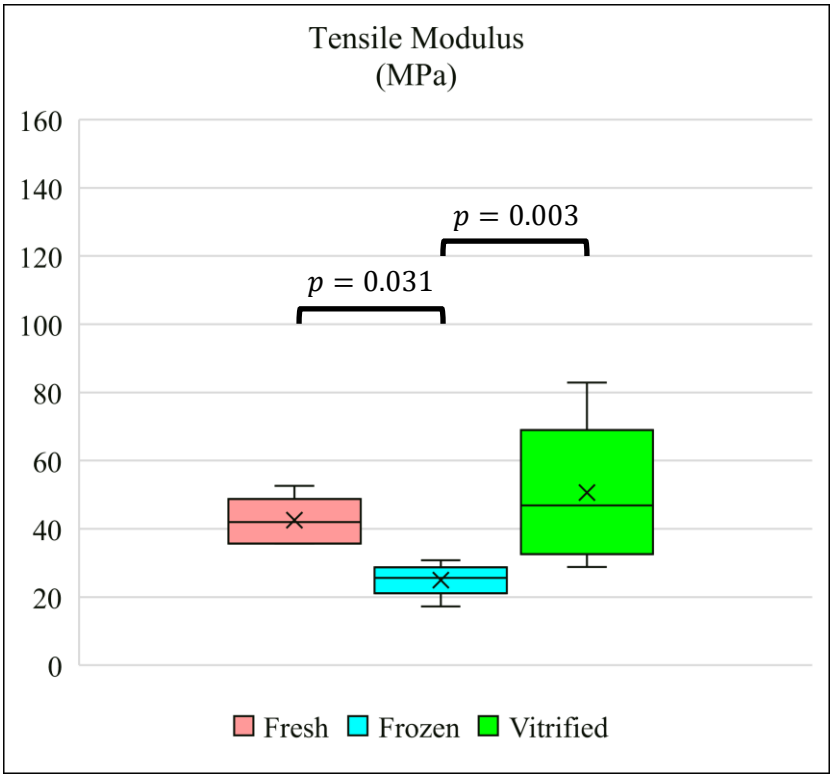

Figure 4-15: Boxplot – Radial Orientation – Tensile Modulus

4.2.5 Orientational Variations in the Tensile Mechanical Properties

To test the first part of the secondary hypothesis that specimens along the circumferential-peripheral orientation would exhibit superior tensile mechanical properties, the tensile mechanical properties along the circumferential-peripheral orientation were compared with that along the circumferential-central, longitudinal, and radial orientations (Figure 4-16, Figure 4-17, and Figure 4-18). To test the second part of the secondary hypothesis that specimens along the radial orientation would exhibit inferior tensile mechanical properties, the tensile mechanical properties along the radial orientation were compared with that along the circumferential-peripheral, circumferential-central, and longitudinal orientations (Figure 4-16, Figure 4-17, and Figure 4-18). ANOVA with linear contrasts was performed for the ultimate tensile stress, failure strain, and tensile modulus between the orientations for each group.

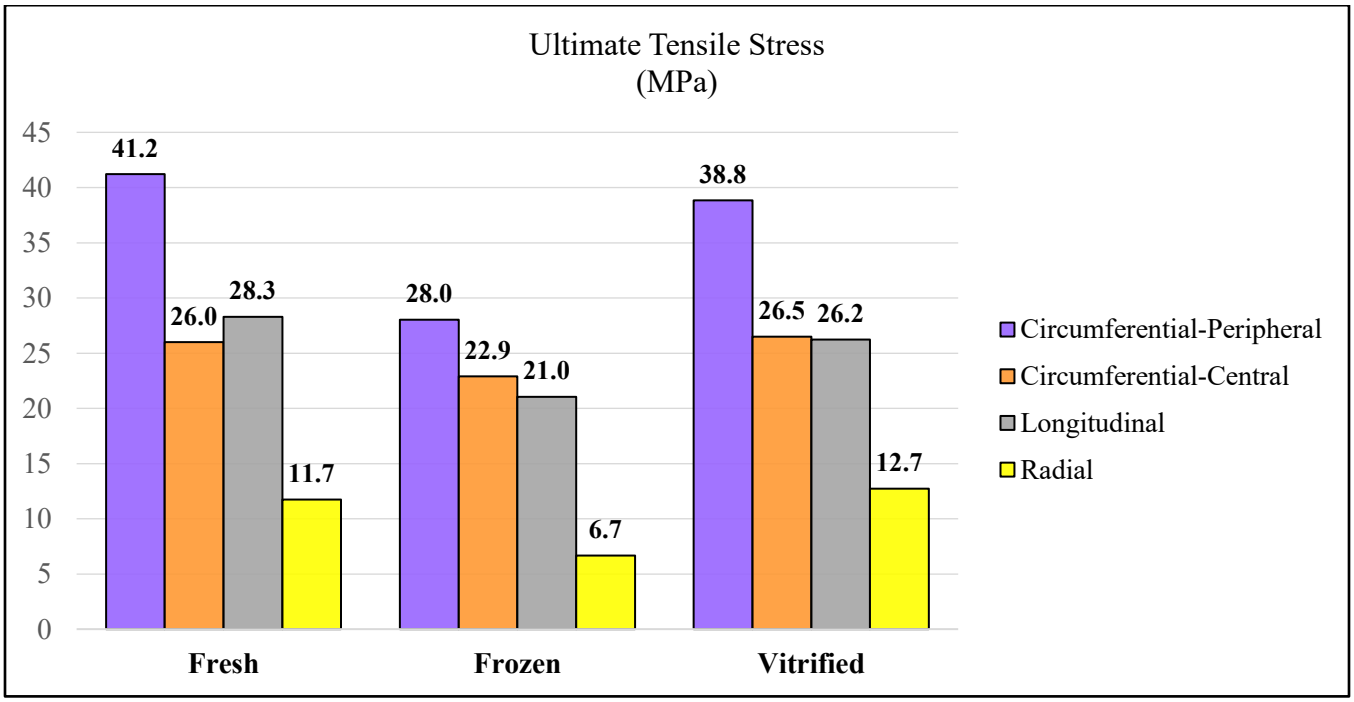

Figure 4-16: Orientational Comparisons – Ultimate Tensile Stress

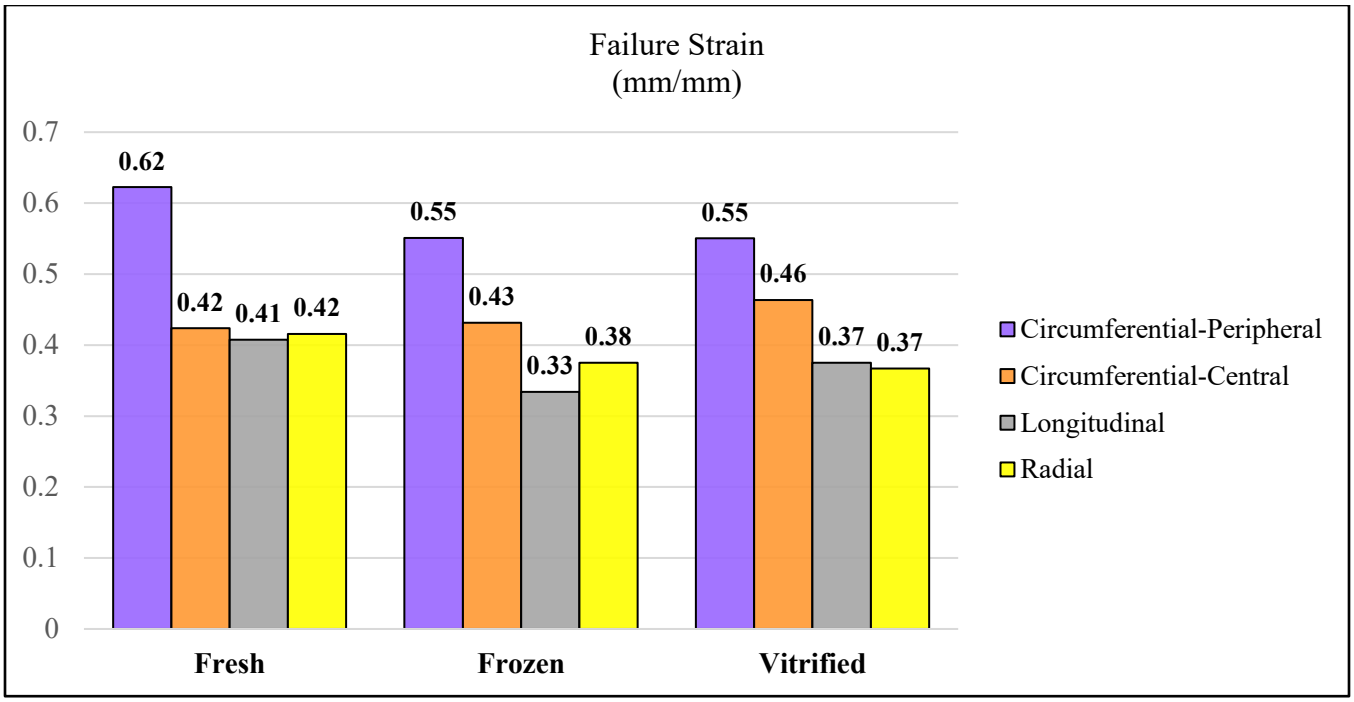

Figure 4-17: Orientational Comparisons – Failure Strain

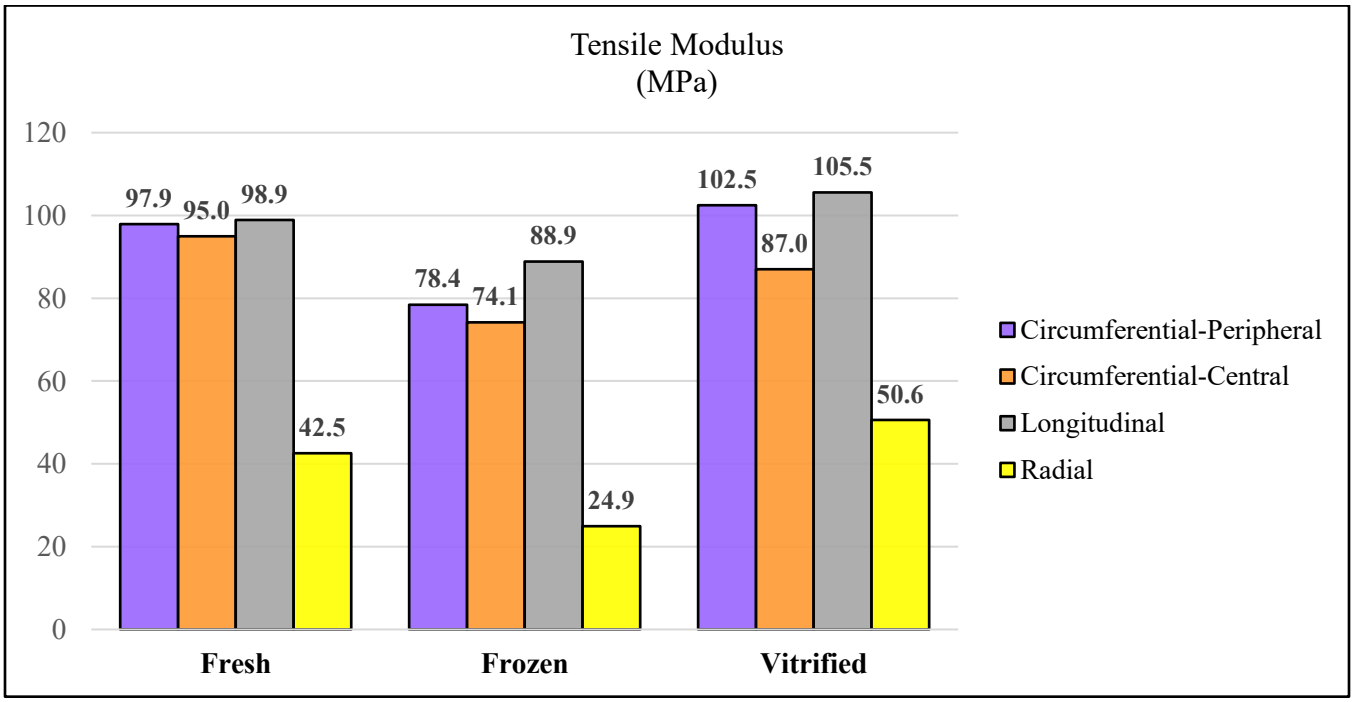

Figure 4-18: Orientational Comparisons – Tensile Modulus

4.2.5.1 Circumferential-Peripheral vs. Circumferential-Central Orientations

For fresh specimens, the ultimate tensile stress ($p < 0.001$) and failure strain ($p < 0.001$) along the circumferential-peripheral orientation were significantly higher than that along the circumferential-central orientation. Similarly, for frozen specimens, the ultimate tensile stress ($p = 0.013$) and failure strain ($p = 0.014$) along the circumferential-peripheral orientation were significantly higher than that along the circumferential-central orientation. Likewise, for vitrified specimens, the ultimate tensile stress ($p < 0.001$) and failure strain ($p = 0.030$) along the circumferential-peripheral orientation were significantly higher than that along the circumferential-central orientation.

4.2.5.2 Circumferential-Peripheral vs. Longitudinal Orientations

For fresh specimens, the ultimate tensile stress ($p < 0.001$) and failure strain ($p < 0.001$) along the circumferential-peripheral orientation were significantly higher than that along the longitudinal orientation. Similarly, for frozen specimens, the ultimate tensile stress ($p = 0.001$) and failure strain ($p < 0.001$) along the circumferential-peripheral orientation were significantly higher than that along the longitudinal orientation. Likewise, for vitrified specimens, the ultimate tensile stress ($p < 0.001$) and failure strain ($p < 0.001$) along the circumferential-peripheral orientation were significantly higher than that along the longitudinal orientation.

4.2.5.3 Circumferential-Peripheral vs. Radial Orientations

For fresh specimens, the ultimate tensile stress ($p < 0.001$), failure strain ($p < 0.001$), and tensile modulus ($p < 0.001$) along the circumferential-peripheral orientation were significantly higher than that along the radial orientation. Similarly, for frozen specimens, the ultimate tensile stress ($p < 0.001$), failure strain ($p < 0.001$), and tensile modulus ($p < 0.001$) along the circumferential-peripheral orientation were significantly higher than that along the radial orientation. Likewise, for vitrified specimens, the ultimate tensile stress ($p < 0.001$), failure strain ($p < 0.001$), and tensile modulus ($p < 0.001$) along the circumferential-peripheral orientation were significantly higher than that along the radial orientation. Furthermore, for fresh and vitrified specimens, the mean tensile modulus along the circumferential-peripheral orientation was approximately 2 times higher than that along the radial orientation. For frozen specimens, the mean tensile modulus along the circumferential-peripheral orientation was approximately 3 times higher than that along the radial orientation.

4.2.5.4 Circumferential-Central vs. Radial Orientations

For fresh specimens, the ultimate tensile stress ($p < 0.001$) and tensile modulus ($p < 0.001$) along the circumferential-central orientation were significantly higher than that along the radial orientation. Likewise, for frozen specimens, the ultimate tensile stress ($p < 0.001$) and tensile modulus ($p < 0.001$) along the circumferential-central orientation were significantly higher than that along the radial orientation. Moreover, for vitrified specimens, the ultimate tensile stress ($p < 0.001$), failure strain ($p = 0.017$), and tensile modulus ($p = 0.007$) along the circumferential-central orientation were significantly higher than that along the radial orientation. Furthermore, for

fresh and vitrified specimens, the mean tensile modulus along the circumferential-central orientation was approximately 2 times higher than that along the radial orientation. For frozen specimens, the mean tensile modulus along the circumferential-central orientation was approximately 3 times higher than that along the radial orientation.

4.2.5.5 Longitudinal vs. Radial Orientations

For fresh specimens, the ultimate tensile stress ($p < 0.001$) and tensile modulus ($p < 0.001$) along the longitudinal orientation were significantly higher than that along the radial orientation. Similarly, for frozen specimens, the ultimate tensile stress ($p < 0.001$) and tensile modulus ($p < 0.001$) along the longitudinal orientation were significantly higher than that along the radial orientation. Likewise, for vitrified specimens, the ultimate tensile stress ($p < 0.001$) and tensile modulus ($p < 0.001$) along the longitudinal orientation were significantly higher than that along the radial orientation. Furthermore, for fresh and vitrified specimens, the mean tensile modulus along the longitudinal orientation was approximately 2 times higher than that along the radial orientation. For frozen specimens, the mean tensile modulus along the longitudinal orientation was approximately 4 times higher than that along the radial orientation.

Chapter 5: Discussion

The experimental results of this research revealed several important findings. The results from unconfined compressive stress-relaxation testing demonstrated that fresh and vitrified menisci exhibit comparable compressive mechanical properties, whereas frozen menisci exhibit inferior compressive mechanical properties in comparison with fresh menisci (significant differences in secant modulus, equilibrium modulus, and instantaneous modulus) and vitrified menisci (significant differences in secant modulus and instantaneous modulus). Moreover, the results from quasi-static tensile testing demonstrated that fresh and vitrified menisci exhibit comparable tensile mechanical properties, whereas frozen menisci exhibit inferior tensile mechanical properties in comparison with fresh and vitrified menisci. Specifically, for circumferential-peripheral specimens, significant differences were identified in the ultimate tensile stress between the fresh and frozen groups, and between the vitrified and frozen groups. For circumferential-central specimens, significant differences were identified in the tensile modulus between the fresh and frozen groups. For longitudinal specimens, significant differences were identified in the ultimate tensile stress and failure strain between the fresh and frozen groups, and in the ultimate tensile stress and tensile modulus between the vitrified and frozen groups. For radial specimens, significant differences were identified in the ultimate tensile stress and tensile modulus between the fresh and frozen groups, and between the vitrified and frozen groups. Furthermore, the results from orientational comparisons indicated that only the ultimate tensile stress and failure strain along the circumferential-peripheral orientation are significantly higher than that along the three other orientations, and only the ultimate tensile stress and tensile modulus along the radial orientation are significantly lower than that along the three other orientations. Besides, the mean

tensile modulus along the circumferential (central and peripheral) and longitudinal orientations are approximately twofold to fourfold higher than that along the radial orientation.

Most of the studies that have quantified the compressive mechanical properties of porcine menisci used frozen porcine menisci. Lakes et al. (2016) performed unconfined compressive stress-relaxation testing on frozen porcine medial menisci. The Young's modulus, instantaneous stress, and steady state stress defined in Lakes and coworkers' study are equivalent to the instantaneous modulus, peak stress, and equilibrium stress in this research, respectively. The Young's modulus ($7.6\ MPa$), instantaneous stress ($0.7\ MPa$), and steady state stress ($0.007\ MPa$) reported in Lakes and coworkers' study are significantly lower than the instantaneous modulus ($32.1 \pm 8.8\ MPa$), peak stress ($3.2 \pm 0.9\ MPa$), and equilibrium stress ($0.02 \pm 0.01\ MPa$) determined in this research. Many differences are identified between Lakes and coworkers' study and this research, including medial meniscus vs. lateral meniscus, storage methods, freezing protocols, compression specimen sizes ($5 \times 3.5\ mm$ vs. $6 \times 2\ mm$), compression specimen locations (central vs. central-posterior), and compression loading protocols (additional 30 cycles of preconditioning in Lakes and coworkers' study particularly). Since the tensile mechanical properties reported in Lakes and coworkers' study are comparable to that in this research, the possible explanation on the dramatic differences between the compressive mechanical properties is limited to different choices of compression specimen size, location, and loading protocol. While frozen porcine menisci are commonly used in quantifying compressive mechanical properties of the meniscal tissue, there has been limited emphasis on fresh porcine menisci. This research involves the investigation on the compressive mechanical properties of fresh porcine menisci,

which creates a baseline for reference in future research. Moreover, while there have been no published studies exploring the effect of preservation techniques on the compressive mechanical properties of the menisci to date, this research investigated the differences in the compressive mechanical properties of fresh, frozen, and vitrified porcine menisci.

The standard deviation ($\pm$ 22.1) of tensile moduli for vitrified circumferential-central specimens are considerably high owing to the presence of a single high tensile modulus (131.2 MPa) which may be attributed to individual differences exhibited between the menisci. Besides, a relatively large difference in the standard deviations of tensile moduli was observed between frozen ($\pm$ 4.8) and vitrified ($\pm$ 20.3) specimens along the radial orientation. The results from the circumferential-central orientation are excluded from the following comparisons since circumferential-central specimens were harvested from the interior of the menisci while specimens along the three other orientations were harvested from the exterior of the menisci. The standard deviations of tensile moduli for frozen circumferential-peripheral and longitudinal specimens fluctuate between $\pm$ 15 to $\pm$ 16, which are higher than that of frozen radial specimens ($\pm$ 4.8). By comparison, the standard deviation ($\pm$ 20.3) of tensile moduli for vitrified radial specimens is reasonable as that of vitrified circumferential-peripheral and longitudinal specimens range from $\pm$ 11 to $\pm$ 27. Therefore, the standard deviation of tensile moduli for frozen radial specimens are considered to be surprisingly low while that of vitrified radial specimens are expected with the presence of individual differences between the menisci. A possible explanation on the dramatically low standard deviation of tensile moduli for frozen radial specimens is that the radial fibers within the meniscal tissue are speculated to be more vulnerable to the alteration in the collagen architecture

caused by the formation of ice crystals during the freezing process, reducing the influence of individual differences exhibited between the menisci.

The tensile mechanical properties of the meniscal tissue have been quantified in many studies on various species including human, bovine, porcine, canine, and ovine. For studies involving porcine menisci, frozen porcine menisci (Abdelgaied et al., 2015; Lakes et al., 2016) were frequently used. In the current research, the experimental results from quasi-static tensile testing demonstrated that frozen longitudinal specimens have a mean ultimate tensile stress of $21.0 \pm 2.6\ MPa$ and a mean tensile modulus of $88.9 \pm 15\ MPa$, while the frozen radial specimens have a mean ultimate tensile stress of $6.7 \pm 1.2\ MPa$ and a mean tensile modulus of $24.9 \pm 4.8\ MPa$. The circumferential specimens in the following studies (Abdelgaied et al., 2015; Lakes et al., 2016) being compared are equivalent to the longitudinal specimens in this research and will be referred to as "comparable to longitudinal" throughout. Abdelgaied et al. (2015) investigated the tensile mechanical properties of frozen porcine medial menisci and reported a mean ultimate tensile stress of approximately $28\ MPa$ and a mean tensile modulus of approximately $135\ MPa$ for comparable to longitudinal specimens. Comparing with the results of frozen longitudinal specimens in this research, Abdelgaied and coworkers reported a higher ultimate tensile stress and tensile modulus. This difference may be attributed to the higher gauge length ($10mm$ vs. $5mm$), the hydrated testing specimens, and the absence of preconditioning in Abdelgaied and coworkers' study. Moreover, Lakes et al. (2016) also evaluated tensile mechanical properties of frozen porcine medial menisci and reported a mean ultimate tensile stress of approximately $24\ MPa$ and a mean tensile modulus of approximately $93\ MPa$ for comparable to longitudinal specimens; and a mean ultimate tensile

stress of approximately 4 MPa and a mean tensile modulus of approximately 14 MPa for radial specimens. Comparing with the results from this research, Lakes and coworkers reported a similar ultimate tensile stress and tensile modulus for comparable to longitudinal specimens and a lower ultimate tensile stress and tensile modulus for radial specimens, which may be owing to the different loading protocols applied between the comparable to longitudinal and radial specimens in Lakes and coworkers' study. While many studies have chosen frozen porcine menisci to quantify the tensile mechanical properties of the meniscal tissue, there has been limited attention on fresh porcine menisci. This research investigated the tensile mechanical properties of fresh porcine menisci, which creates a baseline for reference in future research.

As aforementioned, several studies (Arnoczky et al., 1988; Ahmad et al., 2017) have indicated the effect of freezing and conventional cryopreservation on the tensile mechanical properties of the menisci. Nevertheless, there have been no published studies exploring the effect of vitrification on the tensile mechanical properties of the menisci to date. This research investigated the differences in the mechanical properties of fresh, frozen, and vitrified porcine menisci. The findings of this research demonstrated that fresh and vitrified menisci exhibit comparable mechanical properties, whereas frozen menisci exhibit inferior mechanical properties in comparison with fresh and vitrified menisci. Many studies have revealed that ice formation is lethal to cells (Mcgann & Farrant, 1976; Jomha et al., 2012; Fahy & Wowk, 2015) and results in severe alteration in the structural architecture of the matrix (Jomha et al., 2004; Gelber et al., 2008). Freezing, with the formation of ice crystals, destroys viable cells and alters the collagen network of the meniscus (Gelber et al., 2008), making the meniscus to be more susceptible to injury (Arnoczky et al., 1992).

On the other hand, vitrification, the transformation of an aqueous solution into a non-crystalline amorphous solid (Jomha et al., 2012), inhibits the crystallization of ice (Pegg & Diaper, 1990) and partially preserves cell viability. These may provide a preliminary explanation on the inferior mechanical properties of frozen menisci found in this research compared with fresh and vitrified menisci. Nevertheless, in an effort to gain a better understanding from the clinical perspective on the ultrastructure of the meniscus preserved by freezing or vitrification, histologic examination in conjunction with mechanical testing are recommended for future research. Furthermore, a possible explanation for significant differences identified only in tensile modulus along the circumferential-central orientation between the fresh and frozen groups is that the vitrification time applied in the current treatment protocol is insufficient for the meniscus to achieve complete permeation and thus the internal structure of the tissue may not have been vitrified. For future research, the vitrification protocol can by optimized to further preserve the mechanical properties of vitrified menisci.

The orientational variations in the tensile mechanical properties of the meniscal tissue (Proctor et al., 1989; Tissakht & Ahmed, 1995; Lakes et al., 2016; Peloquin et al., 2016) have been investigated in the literature. The circumferential specimens in the following studies are equivalent to the longitudinal specimens in this research and will be referred to as "comparable to longitudinal" throughout. Proctor et al. (1989) studied frozen bovine medial menisci and found that the mean tensile modulus of comparable to longitudinal specimens are more than thirty times higher than that of radial specimens. The orientational variations between comparable to longitudinal and radial specimens appear to be consistent across species. Studies of frozen medial and lateral human menisci by Tissakht and Ahmed (1995), frozen porcine medial menisci by Lakes et al. (2016), and

frozen bovine medial and lateral menisci by Peloquin et al. (2016) reported that the mean tensile modulus of comparable to longitudinal specimens can be sixfold to tenfold higher than that of radial specimens. While the majority of the studies have focused on the comparison between specimens in the longitudinal and radial directions, this research investigated the differences in the tensile mechanical properties along four different orientations of fresh, frozen, and vitrified porcine lateral menisci. The results of this research demonstrated that the mean tensile modulus of frozen specimens along the circumferential (central and peripheral) and longitudinal orientations are threefold to fourfold higher than that along the radial orientation. Furthermore, the mean tensile modulus of fresh and vitrified specimens along the circumferential (central and peripheral) and longitudinal orientations are approximately two times higher than that along the radial orientation. These results suggest that the radial fibers within the meniscal tissue might be more vulnerable to the alteration in the collagen architecture caused by the formation of ice crystals during the freezing process. Additionally, while the mean ultimate tensile stress and failure strain of circumferential-peripheral specimens are significantly higher than that of specimens along the three other orientations, the mean tensile modulus of circumferential-peripheral specimens are comparable to that of circumferential-central and longitudinal specimens. The predominant circumferentially oriented collagen fibers in the peripheral outmost zone may provide the same stiffness as the collagen fibers in the central zone (i.e. a few radial fibers interwoven between the circumferential fibers) but is capable of withstanding further stress with increased strain.

Meniscal tears are one of the most frequent injuries to the knee and may be classified based on the tear patterns. Common meniscal tear patterns involve vertical longitudinal (including bucket-

handle), horizontal, radial, complex, and degenerative tears. A traumatic vertical longitudinal tear is the most common meniscal tear in young patients (Greis et al., 2002; Lopez-Vidriero & Johnson, 2012). Vertical (from superior to inferior) longitudinal (from anterior to posterior) meniscal tears occur parallel to the circumferential collagen fibers, and a complete and unstable longitudinal tear can become a bucket-handle tear (Brindle et al., 2001; Greis et al., 2002; Lopez-Vidriero & Johnson, 2012). As mentioned previously, the meniscus is compressed and tends to be extruded peripherally as axial loads are generated across the knee during weight bearing. The ultimate tensile stress along the radial orientation was found to be inferior among the three different orientations (i.e. circumferential, longitudinal, and radial) and a longitudinal tear was observed in a ruptured radial tensile specimen. This finding suggests that when the meniscus is undergoing a sudden rotation or high load, the tear would most likely be a longitudinal tear since the collagen fibers along the radial orientation have the lowest failure stress and are more vulnerable to injury. The above speculation is coincident with the fact that vertical longitudinal tears are the most common meniscal tear in younger individuals. Additionally, it is plausible that the ultimate tensile stress and tensile modulus were found to be superior along the circumferential and longitudinal orientations in order for the menisci to play a crucial role in load transmission at the knee.

Chapter 6: Conclusion

6.1 Conclusion

Numerous studies have characterized the behavior of the meniscal tissue under tension and compression. While mechanical testing has been performed on frozen porcine menisci in many studies, there has been limited emphasis on fresh porcine menisci. This research involves the investigation on the compressive and tensile mechanical properties of fresh porcine menisci, which creates a baseline for reference in future research. A small portion of studies have demonstrated the effect of freezing and conventional cryopreservation on only the tensile mechanical properties of the meniscal tissue. Nevertheless, there have been no published studies exploring the effect of vitrification on either the compressive or tensile mechanical properties of the meniscal tissue to date. This research involves the investigation on the compressive and tensile mechanical properties of fresh, frozen, and vitrified porcine lateral menisci. Consistent with the primary hypothesis, fresh and vitrified menisci exhibit comparable mechanical properties, whereas frozen menisci exhibit inferior mechanical properties in comparison with fresh and vitrified menisci. Furthermore, many studies have explored the orientational variations of the meniscal tissue and reported that the tensile modulus of longitudinal specimens can be sixfold to tenfold higher than that of radial specimens across species. While the majority of the studies have concentrated on the comparison between specimens in the longitudinal and radial directions, this research involves the investigation on the variations in the tensile mechanical properties along the circumferential-peripheral, circumferential-central, longitudinal, and radial orientations of fresh, frozen, and vitrified menisci. Inconsistent with the secondary hypothesis, only the ultimate tensile stress and failure strain along the circumferential-peripheral orientation are superior to the three other

orientations, while only the ultimate tensile stress and tensile modulus along the radial orientation are inferior to the three other orientations. Moreover, the mean tensile modulus along the circumferential (central and peripheral) and longitudinal orientations are approximately twofold to fourfold higher than that along the radial orientations.

Cryopreserving meniscal tissue by vitrification has been explored in this research and the findings revealed that vitrification is superior to freezing in preserving mechanical properties of the meniscal tissue. Therefore, vitrification demonstrates a great potential to become a superior meniscal preservation method, offering the patients experienced total meniscectomy an attractive alternative for meniscal transplantation in the future.

6.2 Future Considerations

The current research has several limitations that could be considered and addressed in future testing on the mechanical properties of the menisci. Firstly, a custom designed cutting die can be constructed to achieve consistent specimen thickness. Secondly, instead of measuring the dimensions of each specimen manually with a digital caliper, scanning laser with displacement sensor or photogrammetric technique using a microscope and a digital camera are recommended to further improve the accuracy of dimensional measurements. Moreover, in order to obtain a better understanding on the ultrastructure of the meniscus preserved by freezing and/or vitrification, histologic examination in conjunction with mechanical testing are proposed for future research. Furthermore, the internal structure of the tissue may not have been vitrified since the vitrification

time is insufficient for the meniscus to achieve complete permeation. Therefore, the vitrification protocol can by optimized in future research to further preserve the mechanical properties of the vitrified meniscal tissue.

References

Abdelgaied, A., Stanley, M., Galfe, M., Berry, H., Ingham, E., & Fisher, J. (2015). Comparison of the biomechanical tensile and compressive properties of decellularised and natural porcine meniscus. *Journal of Biomechanics*, *48*(8), 1389–1396. doi: 10.1016/j.jbiomech.2015.02.044

Ahmad, S., Singh, V. A., & Hussein, S. I. (2017). Cryopreservation versus fresh frozen meniscal allograft: A biomechanical comparative analysis. *Journal of Orthopaedic Surgery*, *25*(3), 230949901772794. doi: 10.1177/2309499017727946

Akizuki, S., Mow, V. C., Müller, F., Pita, J. C., Howell, D. S., & Manicourt, D. H. (1986). Tensile properties of human knee joint cartilage: I. Influence of ionic conditions, weight bearing, and fibrillation on the tensile modulus. *Journal of Orthopaedic Research*, *4*(4), 379–392. doi: 10.1002/jor.1100040401

Allen, A. A., Caldwell, G. L., & Fu, F. H. (1995). Anatomy and biomechanics of the meniscus. *Operative Techniques in Orthopaedics*, *5*(1), 2–9. doi: 10.1016/s1048-6666(95)80041-7

Anderson, D. R., Gershuni, D. H., Nakhostine, M., & Danzig, L. A. (1993). The effects of non-weight-bearing and limited motion on the tensile properties of the meniscus. *Arthroscopy: The Journal of Arthroscopic & Related Surgery*, *9*(4), 440–445. doi: 10.1016/s0749-8063(05)80319-6

Andrews, S. H., Rattner, J. B., Shrive, N. G., & Ronsky, J. L. (2015). Swelling significantly affects the material properties of the menisci in compression. *Journal of Biomechanics*, *48*(8), 1485–1489. doi: 10.1016/j.jbiomech.2015.02.001

Andrews, S., Shrive, N., & Ronsky, J. (2011). The shocking truth about meniscus. *Journal of Biomechanics, 44*(16), 2737-2740. doi:10.1016/j.jbiomech.2011.08.026

Arnoczky, S. P., Mcdevitt, C. A., Schmidt, M. B., Mow, V. C., & Warren, R. F. (1988). The effect of cryopreservation on canine menisci: A biochemical, morphologic, and biomechanical evaluation. *Journal of Orthopaedic Research*, *6*(1), 1–12. doi: 10.1002/jor.1100060102

Arnoczky, S. P. (1990). Structure and Biology of the Knee Meniscus. In *Biomechanics of Diarthrodial Joints* (pp. 176–190). New York: Springer-Verlag.

Arnoczky, S. P., Dicarlo, E. F., Obrien, S. J., & Warren, R. F. (1992). Cellular repopulation of deep-frozen meniscal autografts: An experimental study in the dog. *Arthroscopy: The Journal of Arthroscopic & Related Surgery*, *8*(4), 428–436. doi: 10.1016/0749-8063(92)90003-t

Baratz, M. E., Fu, F. H., & Mengato, R. (1986). Meniscal tears: The effect of meniscectomy and of repair on intraarticular contact areas and stress in the human knee. *The American Journal of Sports Medicine*, *14*(4), 270–275. doi: 10.1177/036354658601400405

Bird, M. D., & Sweet, M. B. (1987). A system of canals in semilunar menisci. *Annals of the Rheumatic Diseases*, *46*(9), 670–673. doi: 10.1136/ard.46.9.670

Boyd, K. T., & Myers, P. T. (2003). Meniscus preservation; rationale, repair techniques and results. *The Knee*, *10*(1), 1–11. doi: 10.1016/s0968-0160(02)00147-3

Brindle, T., Nyland, J., & Johnson, D. L. (2001). The meniscus: review of basic principles with application to surgery and rehabilitation. *Journal of Athletic Training*, *36*(2), 160–169.

Bullough, P. G., Munuera, L., Murphy, J., & Weinstein, A. M. (1970). The Strength Of The Menisci Of The Knee As It Relates To Their Fine Structure. *The Journal of Bone and Joint Surgery. British Volume*, *52-B*(3), 564–570. doi: 10.1302/0301-620x.52b3.564

Bursac, P., Arnoczky, S., & York, A. (2009). Dynamic compressive behavior of human meniscus correlates with its extra-cellular matrix composition. *Biorheology*, *46*(3), 227–237. doi: 10.3233/bir-2009-0537

Cox, J. S., Nye, C. E., Schaefer, W. W., & Woodstein, I. J. (1975). The Degenerative Effects of Partial and Total Resection of the Medial Meniscus in Dogs' Knees. *Clinical Orthopaedics and Related Research*, *109*, 178–183. doi: 10.1097/00003086-197506000-00026

Chia, H. N., & Hull, M. L. (2008). Compressive moduli of the human medial meniscus in the axial and radial directions at equilibrium and at a physiological strain rate. *Journal of Orthopaedic Research*, *26*(7), 951–956. doi: 10.1002/jor.20573

Doral, M. N., Bilge, O., Huri, G., Turhan, E., & Verdonk, R. (2018). Modern treatment of meniscal tears. *EFORT Open Reviews*, *3*(5), 260–268. doi: 10.1302/2058-5241.3.170067

Fabbriciani, C., Lucania, L., Milano, G., Panni, A. S., & Evangelisti, M. (1997). Meniscal allografts: cryopreservation vs deep-frozen technique. An experimental study in goats. *Knee Surgery, Sports Traumatology, Arthroscopy*, *5*(2), 124–134. doi: 10.1007/s001670050038

Fahy, G., Macfarlane, D., Angell, C., & Meryman, H. (1984). Vitrification as an approach to cryopreservation. *Cryobiology*, *21*(4), 407–426. doi: 10.1016/0011-2240(84)90079-8

Fahy, G. M., & Wowk, B. (2015). Principles of Cryopreservation by Vitrification. In *Cryopreservation and freeze-drying protocols* (pp. 21–82). New York: Humana Press : Springer. doi: 10.1007/978-1-4939-2193-5

Fairbank, T. J. (1948). Knee Joint Changes After Meniscectomy. *The Journal of Bone and Joint Surgery. British Volume*, *30-B*(4), 664–670. doi: 10.1302/0301-620x.30b4.664

Finger, E. B., & Bischof, J. C. (2018). Cryopreservation by vitrification. *Current Opinion in Organ Transplantation*, *23*(3), 353–360. doi: 10.1097/mot.0000000000000534

Fithian, D. C., Kelly, M. A., & Mow, V. C. (1990). Material Properties and Structure-Function Relationships in the Menisci. *Clinical Orthopaedics and Related Research*, *&NA;*(252). doi: 10.1097/00003086-199003000-00004

Fox, A. J. S., Bedi, A., & Rodeo, S. A. (2011). The Basic Science of Human Knee Menisci. *Sports Health: A Multidisciplinary Approach*, *4*(4), 340–351. doi: 10.1177/1941738111429419

Gabrion, A., Aimedieu, P., Laya, Z., Havet, E., Mertl, P., Grebe, R., & Laude, M. (2005). Relationship between ultrastructure and biomechanical properties of the knee meniscus. *Surgical and Radiologic Anatomy*, *27*(6), 507–510. doi: 10.1007/s00276-005-0031-6

Gelber, P. E., Gonzalez, G., Lloreta, J. L., Reina, F., Caceres, E., & Monllau, J. C. (2008). Freezing causes changes in the meniscus collagen net: a new ultrastructural meniscus disarray

scale. *Knee Surgery, Sports Traumatology, Arthroscopy*, *16*(4), 353–359. doi: 10.1007/s00167-007-0457-y

Gelber, P. E., Gonzalez, G., Torres, R., Giralt, N. G., Caceres, E., & Monllau, J. C. (2009). Cryopreservation does not alter the ultrastructure of the meniscus. *Knee Surgery, Sports Traumatology, Arthroscopy*, *17*(6), 639–644. doi: 10.1007/s00167-009-0736-x

Goertzen, D. J. (1992). A soft tissue test apparatus with application to the knee joint meniscus. M.Sc. thesis, University of Alberta.

Goertzen, D., Budney, D., & Cinats, J. (1997). Methodology and apparatus to determine material properties of the knee joint meniscus. *Medical Engineering & Physics*, *19*(5), 412–419. doi: 10.1016/s1350-4533(97)00011-8

Greis, P. E., Bardana, D. D., Holmstrom, M. C., & Burks, R. T. (2002). Meniscal Injury: I. Basic Science and Evaluation. *Journal of the American Academy of Orthopaedic Surgeons*, *10*(3), 168–176. doi: 10.5435/00124635-200205000-00003

Hayter, A. J. (2013). Descriptive Statistics. In *Probability and statistics for engineers and scientists* (pp. 267-293). Toronto, Canada: Nelson Education.

Jacquet, C., Erivan, R., Argenson, J.-N., Parratte, S., & Ollivier, M. (2018). Effect of 3 Preservation Methods (Freezing, Cryopreservation, and Freezing Irradiation) on Human Menisci Ultrastructure: An Ex Vivo Comparative Study With Fresh Tissue as a Gold Standard. *The American Journal of Sports Medicine*, *46*(12), 2899–2904. doi: 10.1177/0363546518790504

Jomha, N. M., Anoop, P. C., & Mcgann, L. E. (2004). Intramatrix events during cryopreservation of porcine articular cartilage using rapid cooling. *Journal of Orthopaedic Research*, *22*(1), 152–157. doi: 10.1016/s0736-0266(03)00158-x

Jomha, N. M., Elliott, J. A., Law, G. K., Maghdoori, B., Forbes, J. F., Abazari, A., … Mcgann, L. E. (2012). Vitrification of intact human articular cartilage. *Biomaterials*, *33*(26), 6061–6068. doi: 10.1016/j.biomaterials.2012.05.007

Kawamura, S., Lotito, K., & Rodeo, S. A. (2003). Biomechanics and healing response of the meniscus. *Operative Techniques in Sports Medicine*, *11*(2), 68–76. doi: 10.1053/otsm.2003.35899

Kelly, M. A., Fithian, D. C., Chern, K. Y., & Mow, V. C. (1990). Structure and Function of the Meniscus: Basic and Clinical Implications. In *Biomechanics of Diarthrodial Joints* (pp. 191–211). New York: Springer-Verlag.

Lakes, E. H., Matuska, A. M., Mcfetridge, P. S., & Allen, K. D. (2016). Mechanical Integrity of a Decellularized and Laser Drilled Medial Meniscus. *Journal of Biomechanical Engineering*, *138*(3), 1–12. doi: 10.1115/1.4032381

Lechner, K., Hull, M. L., & Howell, S. M. (2000). Is the circumferential tensile modulus within a human medial meniscus affected by the test sample location and cross-sectional area? *Journal of Orthopaedic Research*, *18*(6), 945–951. doi: 10.1002/jor.1100180614

Leslie, B. W., Gardner, D. L., Mcgeough, J. A., & Moran, R. S. (2000). Anisotropic response of the human knee joint meniscus to unconfined compression. *Proceedings of the Institution*

of Mechanical Engineers, Part H: Journal of Engineering in Medicine, *214*(6), 631–635. doi: 10.1243/0954411001535651

Levy, I. M., Torzilli, P. A., & Warren, R. F. (1982). The effect of medial meniscectomy on anterior-posterior motion of the knee. *The Journal of Bone & Joint Surgery*, *64*(6), 883–888. doi: 10.2106/00004623-198264060-00011

Lopez-Vidriero, E., & Johnson, D. H. (2012). Meniscus Resection. In *Operative arthroscopy* (pp. 615–626). Philadelphia: Wolters Kluwer Health. Retrieved from https://ebookcentral.proquest.com

MacConaill, M. A. (1932). The function of intra-articular fibrocartilages, with special reference to the knee and inferior radio-ulnar joints. *Journal of Anatomy*, 210–227.

Majewski, M., Susanne, H., & Klaus, S. (2006). Epidemiology of athletic knee injuries: A 10-year study. *The Knee*, *13*(3), 184–188. doi: 10.1016/j.knee.2006.01.005

Mazur, P. (1970). Cryobiology: The Freezing of Biological Systems. *Science*, *168*(3934), 939–949. doi: 10.1126/science.168.3934.939

Mccarty, E. C., Marx, R. G., & Dehaven, K. E. (2002). Meniscus Repair. *Clinical Orthopaedics and Related Research*, *402*, 122–134. doi: 10.1097/00003086-200209000-00011

McDermott, I. D., Masouros, S. D., Bull, A. M. J., & Amis, A. A. (2010). Anatomy. In *The meniscus* (pp. 11–18). Heidelberg: Springer Verlag.

McDermott, I. D., Masouros, S. D., & Amis, A. A. (2008). Biomechanics of the menisci of the knee. *Current Orthopaedics*, *22*(3), 193–201. doi: 10.1016/j.cuor.2008.04.005

Mcgann, L., & Farrant, J. (1976). Survival of tissue culture cells frozen by a two-step procedure to −196 °C. II. Warming rate and concentration of dimethyl sulphoxide. *Cryobiology*, *13*(3), 269–273. doi: 10.1016/0011-2240(76)90107-3

Mickiewicz, P., Binkowski, M., Bursig, H., & Wro´bel, Z. (2014). Preservation and sterilization methods of the meniscal allografts: literature review. *Cell Tissue Bank* , *15*, 307–317. doi: 10.1007/s10561-013-9396-7

Miller III, R. H., & Azar, F. M. (2007). Knee Injuries. In *Campbell's operative orthopaedics* (11th ed., pp. 2395–2600). Mosby.

Obaid, N., Kortschot, M., & Sain, M. (2017). Understanding the Stress Relaxation Behavior of Polymers Reinforced with Short Elastic Fibers. *Materials*, *10*(5), 472. doi: 10.3390/ma10050472

Pegg, D. E., & Diaper, M. P. (1990). Freezing Versus Vitrification; Basic Principles. In *Cryopreservation and Low Temperature Biology in Blood Transfusion Proceedings of the Fourteenth International Symposium on Blood Transfusion, Groningen 1989, Organised by the Red Cross Blood Bank Groningen-drenthe* (pp. 55–69). Boston: Kluwer Academic Publishers.

Peloquin, J. M., Santare, M. H., & Elliott, D. M. (2016). Advances in Quantification of Meniscus Tensile Mechanics Including Nonlinearity, Yield, and Failure. *Journal of Biomechanical Engineering*, *138*(2). doi: 10.1115/1.4032354

Proctor, C. S., Schmidt, M. B., Whipple, R. R., Kelly, M. A., & Mow, V. C. (1989). Material properties of the normal medial bovine meniscus. *Journal of Orthopaedic Research*, *7*(6), 771–782. doi: 10.1002/jor.1100070602

Rath, E. (2000). The menisci: basic science and advances in treatment. *British Journal of Sports Medicine*, *34*(4), 252–257. doi: 10.1136/bjsm.34.4.252

Rijk, P. C. (2004). Meniscal Allograft Transplantation—Part I: Background, Results, Graft Selection and Preservation, and Surgical Considerations. *Arthroscopy: The Journal of Arthroscopic and Related Surgery*, *20*(7), 728–743. doi: 10.1016/j.arthro.2004.06.015

Sakai, A., & Engelmann, F. (2007). Vitrification, encapsulation-vitrification and droplet-vitrification: a review. *CryoLetters*, *28*(3), 151–172.

Salai, M., Givon, U., Messer, Y., & von Versen, R. (1996). Electron microscopic study on the effects of different preservation methods for meniscal cartilage. *Annals of Transplantation*, *2*(1), 52–54.

Sanchez-Adams, J., & Guilak, F. (2013). Form and Function of the Knee Meniscus. In *Orthopaedic basic science: foundations of clinical practice* (pp. 199–211). Rosemont: American academy of orthopaedic surgeons.

Seedhom, B. B., Dowson, D., & Wright, V. (1974). Proceedings: Functions of the menisci. A preliminary study. *Annals of the Rheumatic Diseases*, *33*(1), 111–111. doi: 10.1136/ard.33.1.111

Skaggs, D. L., Warden, W. H., & Mow, V. C. (1994). Radial tie fibers influence the tensile properties of the bovine medial meniscus. *Journal of Orthopaedic Research*, *12*(2), 176–185. doi: 10.1002/jor.1100120205

Stapleton, T. W., Ingram, J., Katta, J., Knight, R., Korossis, S., Fisher, J., & Ingham, E. (2008). Development and Characterization of an Acellular Porcine Medial Meniscus for Use in Tissue Engineering. *Tissue Engineering Part A*, *14*(4), 505–518. doi: 10.1089/tea.2007.0233

Sweigart, M. A., & Athanasiou, K. A. (2005). Tensile and Compressive Properties of the Medial Rabbit Meniscus. *Proceedings of the Institution of Mechanical Engineers, Part H: Journal of Engineering in Medicine*, *219*(5), 337–347. doi: 10.1243/095441105x34329

Sweigart, M. A., Zhu, C. F., Burt, D. M., Deholl, P. D., Agrawal, C. M., Clanton, T. O., & Athanasiou, K. A. (2004). Intraspecies and Interspecies Comparison of the Compressive Properties of the Medial Meniscus. *Annals of Biomedical Engineering*, *32*(11), 1569–1579. doi: 10.1114/b:abme.0000049040.70767.5c

Takroni, T., Laouar, L., Adesida, A., Elliott, J. A. W., & Jomha, N. M. (2016). Anatomical study: comparing the human, sheep and pig knee meniscus. *Journal of Experimental Orthopaedics*, *3*(1). doi: 10.1186/s40634-016-0071-3

Tissakht, M., & Ahmed, A. (1995). Tensile stress-strain characteristics of the human meniscal material. *Journal of Biomechanics*, *28*(4), 411–422. doi: 10.1016/0021-9290(94)00081-e

Verdonk, R., & Kohn, D. (1999). Harvest and conservation of meniscal allografts. *Scandinavian Journal of Medicine & Science in Sports*, *9*(3), 158–159. doi: 10.1111/j.1600-0838.1999.tb00446.x

Voloshin, A. S., & Wosk, J. (1983). Shock absorption of meniscectomized and painful knees: A comparative in vivo study. *Journal of Biomedical Engineering*, *5*(2), 157–161. doi: 10.1016/0141-5425(83)90036-5

Appendix A: Experimental Results

A.1 Compressive Mechanical Properties

Compressive mechanical properties including the peak stress (MPa) and secant modulus (MPa), equilibrium stress (MPa) and equilibrium modulus (MPa), instantaneous modulus (MPa), and percent stress relaxation ($\%$) are tabulated in Table A-1 for the fresh group, Table A-2 for the frozen group, and Table A-3 for the vitrified group.

Table A-1: Compressive Mechanical Properties of Fresh Group

Test Group		Peak Stress *(MPa)*	Secant Modulus *(MPa)*	Equilibrium Stress *(MPa)*	Equilibrium Modulus *(MPa)*	Instantaneous Modulus *(MPa)*	Percent Relaxation *(%)*
Fresh	1	-3.8	25.3	-0.02	0.13	38.1	99.5
	2	-4.6	30.5	-0.03	0.18	48.1	99.4
	3	-5.5	36.8	-0.06	0.39	56.0	98.9
	4	-4.5	30.1	-0.01	0.10	46.5	99.7
	5	-5.8	38.4	-0.13	0.84	55.4	97.8
	6	-5.4	36.4	-0.13	0.84	54.1	97.7
	7	-5.1	34.0	-0.02	0.14	50.5	99.6
	8	-4.4	29.4	-0.01	0.10	45.2	99.7
	9	-4.5	29.7	-0.03	0.19	45.5	99.4
	10	-4.9	32.5	-0.04	0.26	49.6	99.2
	11	-4.9	32.8	-0.04	0.25	47.9	99.2
	12	-5.0	33.5	-0.02	0.14	51.4	99.6

Table A-2: Compressive Mechanical Properties of Frozen Group

Test Group		Peak Stress *(MPa)*	Secant Modulus *(MPa)*	Equilibrium Stress *(MPa)*	Equilibrium Modulus *(MPa)*	Instantaneous Modulus *(MPa)*	Percent Relaxation *(%)*
Frozen	1	-2.0	13.1	-0.02	0.15	18.8	98.8
	2	-3.9	26.3	-0.02	0.11	40.8	99.6
	3	-4.9	32.6	-0.01	0.10	47.3	99.7
	4	-4.1	27.8	-0.02	0.11	40.9	99.6
	5	-3.0	20.2	-0.02	0.15	32.6	99.3
	6	-3.0	19.7	-0.05	0.33	29.0	98.3
	7	-3.0	19.7	-0.21	1.43	29.5	92.7
	8	-2.4	16.2	-0.02	0.15	29.8	99.1
	9	-3.4	22.7	-0.03	0.19	33.5	99.2
	10	-2.4	16.4	-0.01	0.04	23.7	99.8
	11	-2.7	17.9	-0.03	0.17	25.5	99.0
	12	-2.7	18.0	-0.01	0.05	27.8	99.7

Table A-3: Compressive Mechanical Properties of Vitrified Group

Test Group		Peak Stress *(MPa)*	Secant Modulus *(MPa)*	Equilibrium Stress *(MPa)*	Equilibrium Modulus *(MPa)*	Instantaneous Modulus *(MPa)*	Percent Relaxation *(%)*
Vitrified	1	-4.0	26.7	-0.03	0.20	39.8	99.3
	2	-5.1	34.3	-0.03	0.22	51.4	99.4
	3	-3.3	21.8	-0.03	0.19	33.7	99.1
	4	-4.7	31.6	-0.02	0.16	46.7	99.5
	5	-4.4	29.2	-0.03	0.20	43.9	99.3
	6	-3.5	23.1	-0.09	0.63	33.1	97.3
	7	-3.8	25.5	-0.19	1.24	37.7	95.1
	8	-3.5	23.3	-0.25	1.69	34.6	92.7
	9	-4.7	31.2	-0.02	0.11	47.3	99.6
	10	-4.9	32.5	-0.02	0.16	48.6	99.5
	11	-4.0	26.4	-0.02	0.12	39.5	99.6
	12	-4.2	27.7	-0.02	0.15	40.6	99.5

A.1.2 Three-Term Prony Series

From the 3-term Prony series model, three relaxation time constants (τ_1, τ_2, τ_3) of each specimen are tabulated in Table A-4 for the fresh group, Table A-5 for the frozen group, and Table A-6 for the vitrified group.

Table A-4: Three Relaxation Time Constants of Fresh Group

Test Group		τ_1 (s)	τ_2 (s)	τ_3 (s)	R^2
Fresh	1	2.5	16.1	123.5	99.9%
	2	2.7	16.3	120.9	100.0%
	3	4.5	23.9	131.3	100.0%
	4	2.8	14.7	96.4	100.0%
	5	3.6	20.6	143.2	100.0%
	6	2.6	15.9	110.0	99.9%
	7	2.7	16.0	106.5	100.0%
	8	2.9	15.7	103.1	100.0%
	9	4.0	20.4	128.2	100.0%
	10	3.6	20.4	129.3	100.0%
	11	4.2	22.0	132.4	100.0%
	12	3.1	17.1	118.5	100.0%

Table A-5: Three Relaxation Time Constants of Frozen Group

Test Group		τ_1 (s)	τ_2 (s)	τ_3 (s)	R^2
Frozen	1	3.3	20.5	121.5	100.0%
	2	2.9	16.3	104.9	100.0%
	3	2.5	14.8	106.1	99.9%
	4	2.1	14.2	114.5	99.9%
	5	3.0	17.3	113.4	100.0%
	6	2.3	17.8	226.2	99.8%
	7	2.9	17.8	139.6	99.9%
	8	3.3	18.2	122.7	100.0%
	9	3.3	19.0	114.7	100.0%
	10	1.6	10.6	87.1	99.9%
	11	3.6	22.9	148.8	100.0%
	12	2.2	13.4	104.0	99.9%

Table A-6: Three Relaxation Time Constants of Vitrified Group

Test Group		τ_1 (s)	τ_2 (s)	τ_3 (s)	R^2
Vitrified	1	2.9	17.2	117.8	100.0%
	2	3.7	19.6	117.4	100.0%
	3	2.5	15.3	99.8	100.0%
	4	2.5	15.9	116.6	99.9%
	5	3.2	19.1	125.2	100.0%
	6	2.7	21.1	391.3	99.8%
	7	2.9	16.1	115.2	99.9%
	8	3.9	21.8	145.7	100.0%
	9	3.2	16.5	104.4	100.0%
	10	3.3	17.2	107.6	100.0%
	11	3.2	16.9	108.9	100.0%
	12	3.4	19.1	121.8	100.0%

A.2 Tensile Mechanical Properties

A.2.1 Tensile Mechanical Properties along Circumferential-Peripheral Orientation

Tensile mechanical properties along the circumferential-peripheral orientation including the ultimate tensile stress (MPa), failure strain (mm/mm), and tensile modulus (MPa) are tabulated in Table A-7 for each group.

Table A-7: Tensile Mechanical Properties – Circumferential-Peripheral Orientation

Test Group		Ultimate Tensile Stress *(MPa)*	Failure Strain *(mm/mm)*	Tensile Modulus *(MPa)*
Fresh	1	41.3	0.76	86.3
	2	32.3	0.65	74.9
	3	33.0	0.61	72.0
	4	44.5	0.46	119.3
	5	42.4	0.68	100.9
	6	53.9	0.57	134.2
Frozen	1	23.7	0.70	60.4
	2	31.1	0.49	98.0
	3	22.5	0.45	68.6
	4	35.2	0.52	97.6
	5	30.9	0.61	76.5
	6	24.9	0.54	69.4
Vitrified	1	34.7	0.62	79.1
	2	31.0	0.52	77.6
	3	49.5	0.62	118.7
	4	36.8	0.62	79.5
	5	46.0	0.50	136.3
	6	35.1	0.43	123.7

A.2.2 Tensile Mechanical Properties along Circumferential-Central Orientation

Tensile mechanical properties along the circumferential-central orientation including the ultimate tensile stress (MPa), failure strain (mm/mm), and tensile modulus (MPa) are tabulated in Table A-8 for each group.

Table A-8: Tensile Mechanical Properties – Circumferential-Central Orientation

Test Group		Ultimate Tensile Stress *(MPa)*	Failure Strain *(mm/mm)*	Tensile Modulus *(MPa)*
Fresh	1	33.7	0.58	94.3
	2	22.2	0.38	96.4
	3	33.1	0.46	102.2
	4	20.4	0.38	81.3
	5	22.2	0.40	91.6
	6	24.5	0.36	104.0
Frozen	1	26.7	0.54	67.0
	2	25.5	0.50	65.6
	3	22.1	0.36	79.4
	4	22.2	0.46	74.2
	5	18.8	0.35	71.8
	6	22.2	0.38	87.0
Vitrified	1	25.0	0.60	77.9
	2	27.0	0.47	78.6
	3	20.4	0.39	72.9
	4	25.2	0.49	75.0
	5	28.3	0.47	86.3
	6	33.1	0.37	131.2

A.2.3 Tensile Mechanical Properties along Longitudinal Orientation

Tensile mechanical properties along the longitudinal orientation including the ultimate tensile stress (MPa), failure strain (mm/mm), and tensile modulus (MPa) are tabulated in Table A-9 for each group.

Table A-9: Tensile Mechanical Properties – Longitudinal Orientation

Test Group		Ultimate Tensile Stress *(MPa)*	Failure Strain *(mm/mm)*	Tensile Modulus *(MPa)*
Fresh	1	20.1	0.34	93.1
	2	29.4	0.37	100.6
	3	33.2	0.49	105.0
	4	31.8	0.47	98.6
	5	26.7	0.36	95.7
	6	28.7	0.41	100.4
Frozen	1	23.9	0.34	103.7
	2	20.2	0.29	92.8
	3	20.9	0.34	91.3
	4	17.5	0.36	59.8
	5	24.3	0.35	92.3
	6	19.6	0.32	93.4
Vitrified	1	20.8	0.30	99.9
	2	27.5	0.41	112.8
	3	29.1	0.37	116.5
	4	25.7	0.43	102.7
	5	30.6	0.38	113.7
	6	23.7	0.37	87.6

A.2.4 Tensile Mechanical Properties along Radial Orientation

Tensile mechanical properties along the radial orientation including the ultimate tensile stress (MPa), failure strain (mm/mm), and tensile modulus (MPa) are tabulated in Table A-10 for each group.

Table A-10: Tensile Mechanical Properties – Radial Orientation

Test Group		Ultimate Tensile Stress *(MPa)*	Failure Strain *(mm/mm)*	Tensile Modulus *(MPa)*
Fresh	1	15.3	0.47	47.2
	2	10.8	0.37	47.5
	3	11.6	0.35	52.6
	4	12.9	0.49	35.6
	5	9.3	0.41	36.8
	6	10.5	0.41	35.6
Frozen	1	7.9	0.52	17.2
	2	7.4	0.40	28.1
	3	6.9	0.38	27.1
	4	4.6	0.26	22.4
	5	5.8	0.29	30.7
	6	7.5	0.39	24.1
Vitrified	1	6.9	0.40	28.8
	2	9.9	0.37	33.8
	3	11.1	0.41	41.8
	4	17.8	0.30	82.9
	5	12.5	0.34	52.0
	6	18.3	0.38	64.3

Appendix B: Outliers

B.1 Compressive Mechanical Properties

Outliers of the peak stress (Figure B-1) and secant modulus (Figure B-2), equilibrium stress (Figure B-3) and equilibrium modulus (Figure B-4), instantaneous modulus (Figure B-5), and percent relaxation (Figure B-6) in each group were identified with the boxplot.

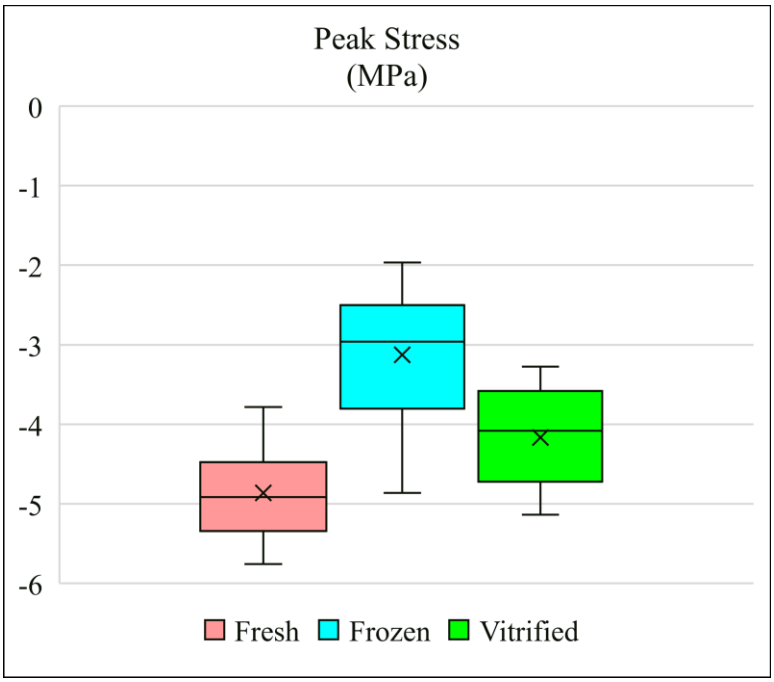

Figure B-1: Boxplot – Peak Stress

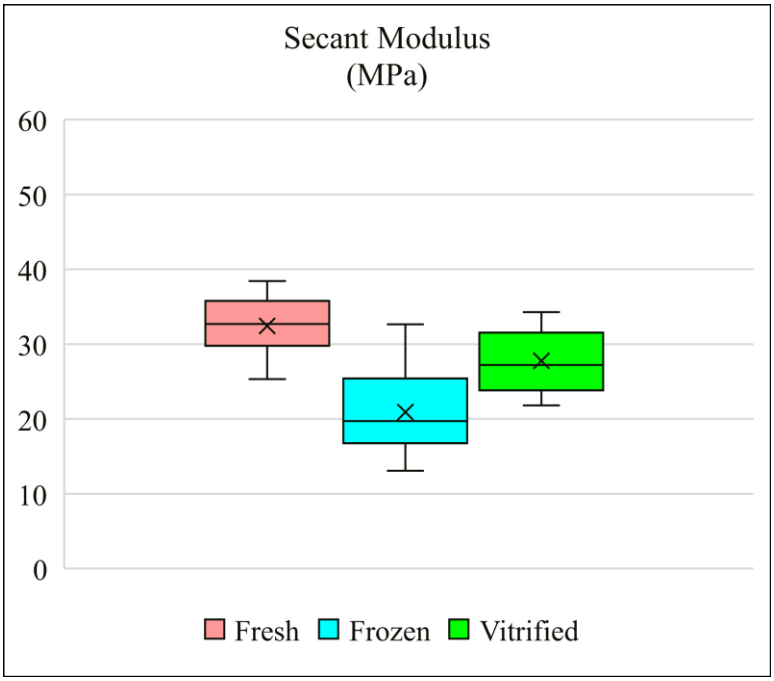

Figure B-2: Boxplot – Secant Modulus

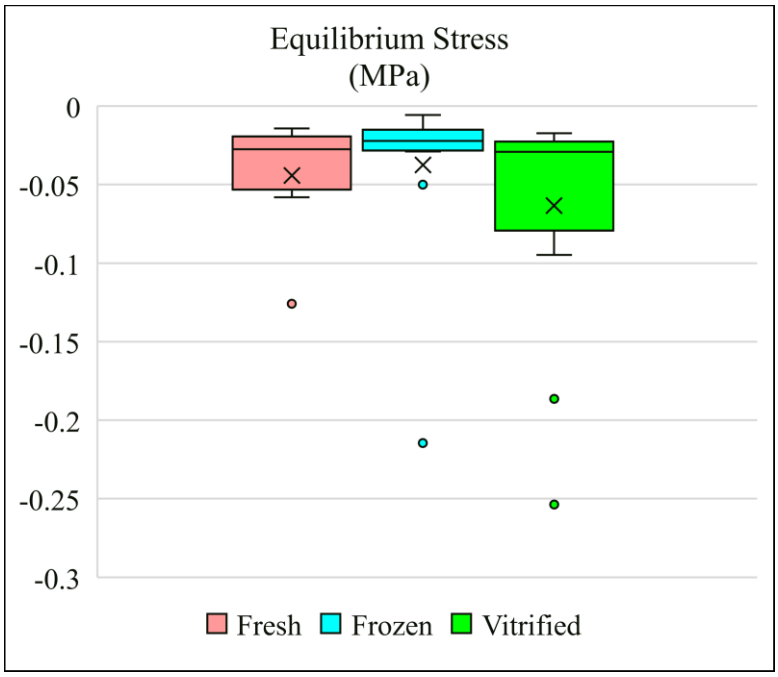

Figure B-3: Boxplot – Equilibrium Stress

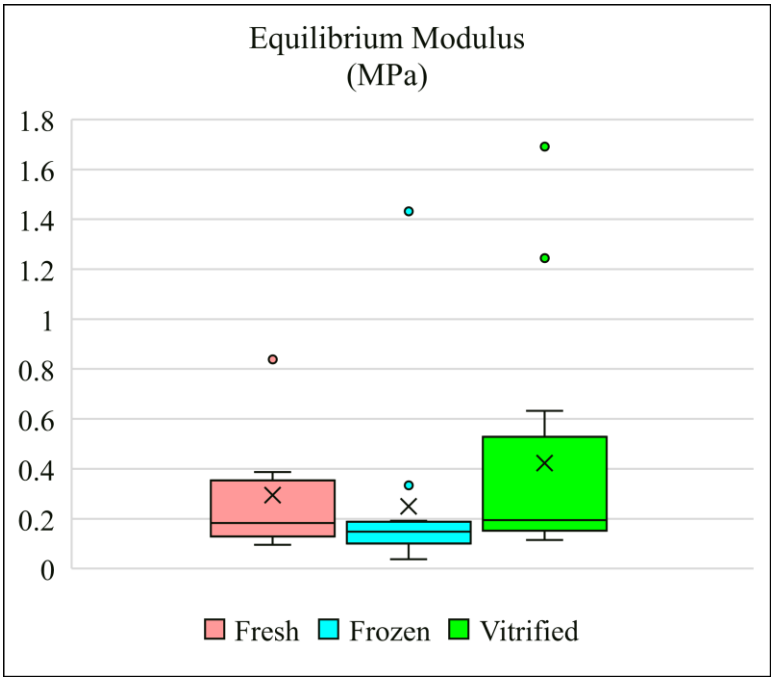

Figure B-4: Boxplot – Equilibrium Modulus

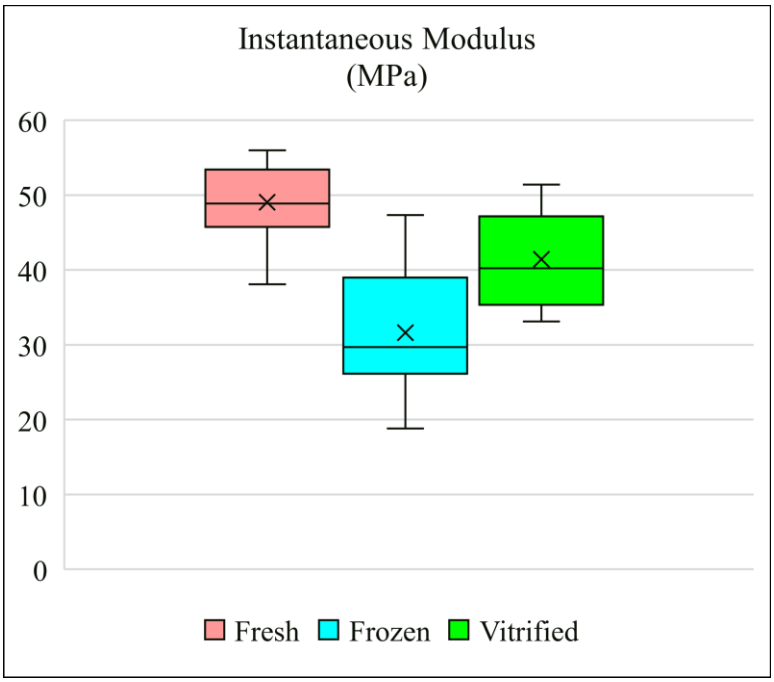

Figure B-5: Boxplot – Instantaneous Modulus

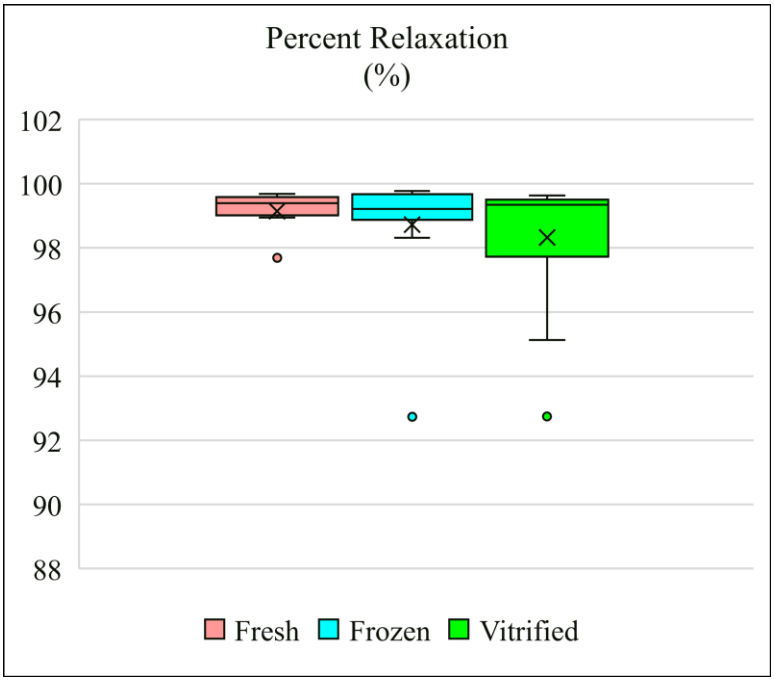

Figure B-6: Boxplot – Percent Relaxation

B.1.2 Three-Term Prony Series

Outliers of the first relaxation time constant (Figure B-7), second relaxation time constant (Figure B-8), and third relaxation time constant (Figure B-9) in each group were identified with the boxplot.

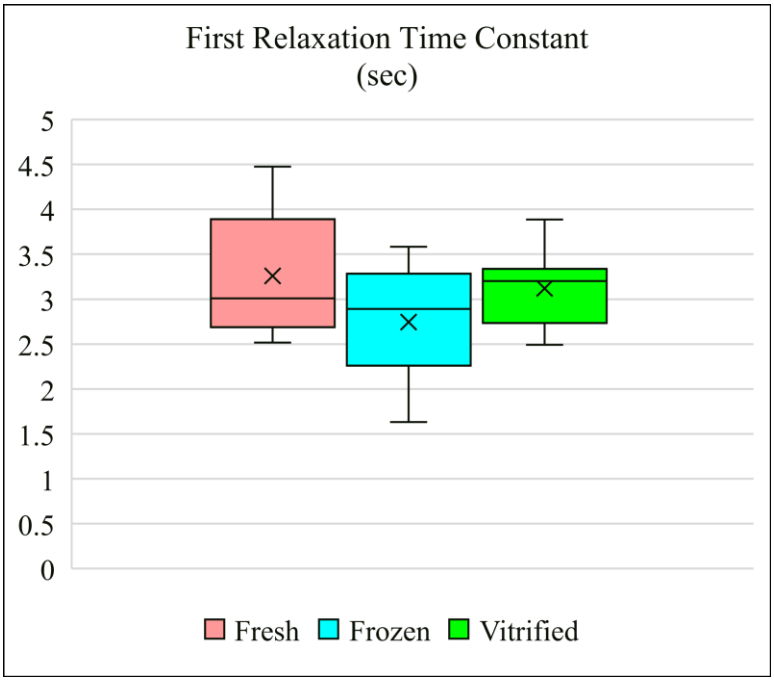

Figure B-7: Boxplot – First Relaxation Time Constant

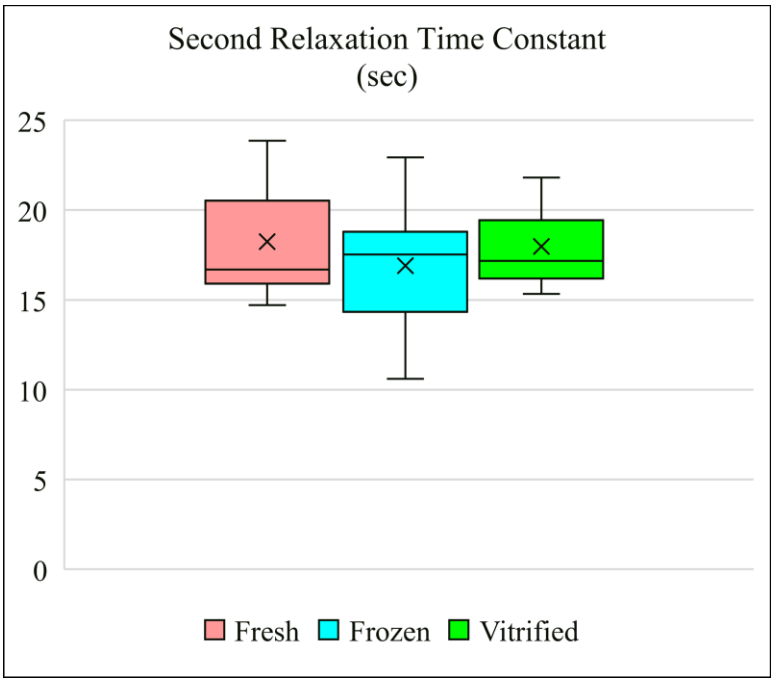

Figure B-8: Boxplot – Second Relaxation Time Constant

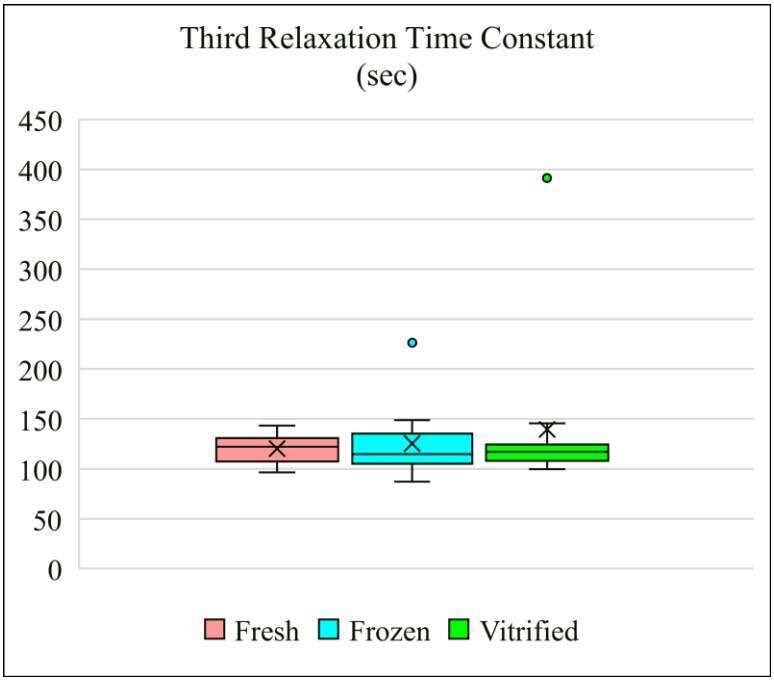

Figure B-9: Boxplot – Third Relaxation Time Constant

B.2 Tensile Mechanical Properties

B.2.1 Tensile Mechanical Properties along Longitudinal Orientation without the Outlier

The mean and standard deviation (SD) values of the tensile mechanical properties along the longitudinal orientation without the outlier for fresh ($n = 6$), frozen ($n = 5$), and vitrified ($n = 6$) groups are presented in Table B-1. The boxplots excluding the outlier in the frozen group of the ultimate tensile stress (MPa), failure strain (mm/mm), and tensile modulus (MPa) along the longitudinal orientation are shown in Figure B-10, Figure B-11, and Figure B-12 respectively.

Table B-1: Mean and Standard Deviation of Tensile Mechanical Properties along Longitudinal Orientation without the Outlier

Test Group	Descriptive Statistics	Ultimate Tensile Stress (MPa)	Failure Strain (mm/mm)	Tensile Modulus (MPa)
Fresh	Mean	28.3	0.41	98.9
	SD	4.6	0.06	4.2
Frozen	Mean	21.8	0.33	94.7
	SD	2.2	0.02	5.1
Vitrified	Mean	26.2	0.37	105.5
	SD	3.6	0.04	11.0

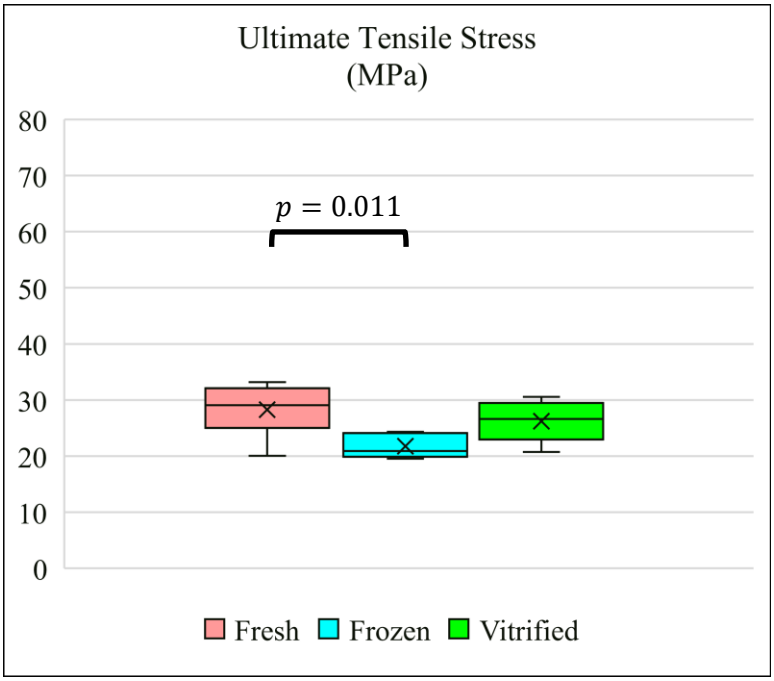

Figure B-10: Boxplot – Longitudinal Orientation without the Outlier – Ultimate Tensile Stress

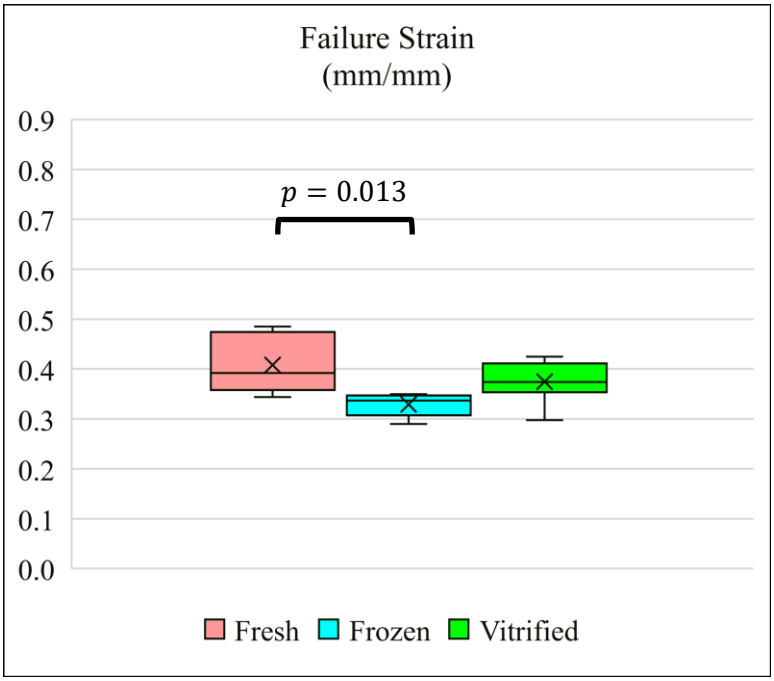

Figure B-11: Boxplot – Longitudinal Orientation without the Outlier – Failure Strain

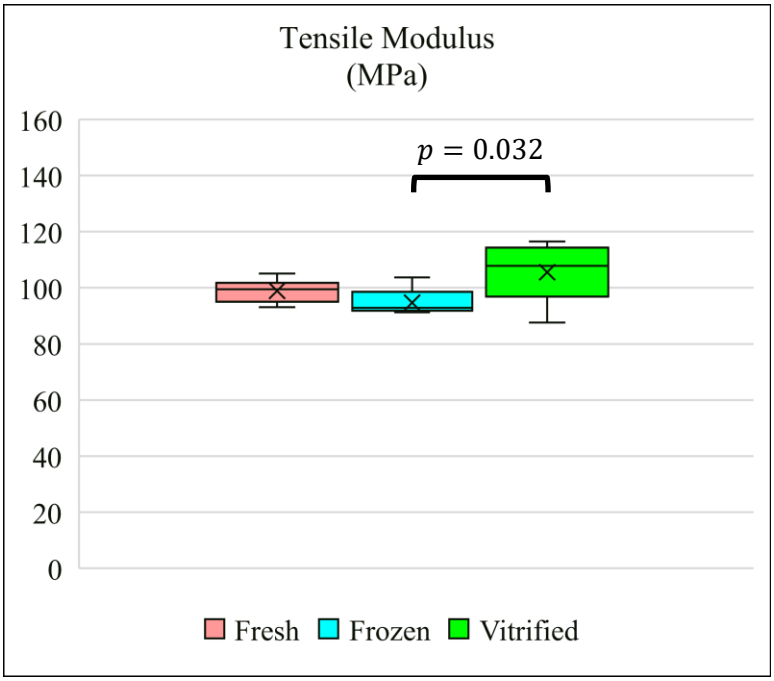

Figure B-12: Boxplot – Longitudinal Orientation without the Outlier – Tensile Modulus